Journal of Biological Engineering

RESEARCH

Open Access

Integrative analysis of gene expression, protein abundance, and metabolomic profiling elucidates complex relationships in chronic hyperglycemia-induced changes in human aortic smooth muscle cells

Smriti Bohara[1], Atefeh Bagheri[2], Elif G. Ertugral[1], Igor Radzikh[3], Yana Sandlers[3], Peng Jiang[2,4,5*] and Chandrasekhar R. Kothapalli[1*]

Abstract

Type 2 diabetes mellitus (T2DM) is a major public health concern with significant cardiovascular complications (CVD). Despite extensive epidemiological data, the molecular mechanisms relating hyperglycemia to CVD remain incompletely understood. We here investigated the impact of chronic hyperglycemia on human aortic smooth muscle cells (HASMCs) cultured under varying glucose conditions in vitro, mimicking normal (5 mmol/L), pre-diabetic (10 mmol/L), and diabetic (20 mmol/L) conditions, respectively. Normal HASMC cultures served as baseline controls, and patient-derived T2DM-SMCs served as disease controls. Results showed significant increases in cellular proliferation, area, perimeter, and F-actin expression with increasing glucose concentration ($p < 0.01$), albeit not exceeding the levels in T2DM cells. Atomic force microscopy analysis revealed significant decreases in Young's moduli, membrane tether forces, membrane tension, and surface adhesion in SMCs at higher glucose levels ($p < 0.001$), with T2DM-SMCs being the lowest among all the cases ($p < 0.001$). T2DM-SMCs exhibited elevated levels of selected pro-inflammatory markers (e.g., ILs-6, 8, 23; MCP-1; M-CSF; MMPs-1, 2, 3) compared to glucose-treated SMCs ($p < 0.01$). Conversely, growth factors (e.g., VEGF-A, PDGF-AA, TGF-β1) were higher in SMCs exposed to high glucose levels but lower in T2DM-SMCs ($p < 0.01$). Pathway enrichment analysis showed significant increases in the expression of inflammatory cytokine-associated pathways, especially involving IL-10, IL-4 and IL-13 signaling in genes that are up-regulated by elevated glucose levels. Differentially regulated gene analysis showed that compared to SMCs receiving normal glucose, 513 genes were upregulated and 590 genes were downregulated in T2DM-SMCs; fewer genes were differentially expressed in SMCs receiving higher glucose levels. Finally, the altered levels in genes involved in ECM organization, elastic fiber synthesis and formation, laminin interactions, and ECM proteoglycans were identified. Growing literature suggests that phenotypic switching in SMCs lead to arterial

*Correspondence:
Peng Jiang
p.jiang@csuohio.edu
Chandrasekhar R. Kothapalli
c.kothapalli@csuohio.edu

Full list of author information is available at the end of the article

wall remodeling (e.g., change in stiffness, calcific deposits formation), with direct implications in the onset of CVD complications. Our results suggest that chronic hyperglycemia is one such factor that leads to morphological, biomechanical, and functional alterations in vascular SMCs, potentially contributing to the pathogenesis of T2DM-associated arterial remodeling. The observed differences in gene expression patterns between in vitro hyperglycemic models and patient-derived T2DM-SMCs highlight the complexity of T2DM pathophysiology and underline the need for further studies.

Keywords Hyperglycemia, Biomechanics, Vascular smooth muscle cells, Diabetes, Gene expression, Transcriptomics, Pathway analysis

Introduction

T2DM is a serious public health concern and a global burden. It is one of the leading causes of mortality affecting more than half a billion people worldwide, and directly contributing to at least a few million deaths annually [1]. T2DM detection is difficult in its early stages leaving many people undiagnosed, and often independently leads to the onset of CVD by the time of diagnosis [2–4] T2DM is a chronic metabolic and inflammatory condition, marked by inadequate insulin secretion by pancreatic β-cells and gradual buildup of tissue insulin resistance, with significant implications in accelerated vascular aging and CVD [5, 6]. T2DM is a complex multifactorial disease and has been implicated in the onset of coronary and peripheral artery diseases (e.g., atherosclerosis, stroke), microvascular (e.g., retinopathy, nephropathy) and neuropathic complications, hypertension, dyslipidemia, and arterial stiffness [7].

When the insulin secretion in diabetic patients cannot maintain glucose homeostasis, it results in hyperglycemia, hyperinsulinemia, inflammation, and higher body fat content, which in turn dysregulate the immune system, adipokines, gut microbiota, and a host of other tissue functions, resulting in arterial remodeling and CVD [8]. Despite its prevalence and the availability of epidemiological data related to T2DM pathophysiology, the molecular mechanisms by which hyperglycemia contributes to CVD are still being elucidated [9, 10]. In healthy vasculature, ECs play a crucial role in maintaining vessel homeostasis and VSMC contractile phenotype by releasing numerous factors (e.g., VEGF, NO). T2DM conditions lead to endothelial dysfunction, release of various inflammatory markers (e.g., ROS, interleukins, TNF-α), and elevated oxidative stress that disturbs this homeostasis and activates SMCs, resulting in vasoconstriction, thrombus formation, arterial remodeling, and the onset of CVD [11–14]. When the functioning EC layer is compromised, VSMCs are exposed to high glucose levels in their microenvironment and the glucose molecules could easily pass through their cell membrane leading to intracellular hyperglycemia and their dedifferentiation [15–17]. Elucidating the role of chronic higher glucose levels on VSMC phenotype and genotype could offer insights into the fundamental mechanisms by which hyperglycemia progresses and offer therapeutic avenues for modulating undesirable outcomes.

The direct contribution of any singular factor on T2DM complications is hard to isolate in both humans and animal models, especially that of hyperglycemic levels. VSMCs cultured in vitro in high glucose conditions (≥20 mmol/L) exhibited proliferation, migration, adhesion, necrosis via H_2O_2 formation, and elevated secretion of various biomolecules (e.g., ROS, TNF-α, MMP-2), along with activation of numerous pathways (e.g., JNK, ERK, AKT, NF-κB, MAPK) [18–23]. In these cultures, cells were typically exposed to high glucose levels for a short duration (3 –72 h), or rodent SMCs were used in lieu of human cells, which do not efficiently mimic the chronic buildup of high blood glucose levels in humans in vivo. The potential benefits of numerous drugs tested in such studies to regulate VSMC behavior in vitro or in animal models in vivo have not led to breakthroughs in clinical trials, suggesting that a deeper understanding of the co-expression between metabolomic, transcriptomic, and proteomic transformations in these cells under prolonged exposure to elevated glucose concentrations mimicking pre-diabetic and diabetic conditions is critical to delineate the specific role of high glucose levels in T2DM-initiated arterial remodeling.

In this study, we investigated the role of hyperglycemic conditions on the activation of VSMC pathways that contribute to early onset of endothelial dysfunction and arterial remodeling. We cultured human aortic smooth muscle cells (HASMCs; isolated from multiple donors) for 21 days to broadly mimic normal (5 mmol/L glucose), prediabetic (10 mmol/L glucose), and diabetic (20 mmol/L glucose) states. The phenotypic and biomechanical changes in cells under these conditions were assessed using AFM and confocal imaging. Metabolomic, proteomic, and RNA-seq analysis were performed to compare with those from human T2DM–HASMCs. Our study reveals the biological pathways activated during early stages of T2DM and identifies crucial biomarkers triggered during hyperglycemic conditions.

Methodology

Cell cultures

Cryopreserved HASMCs from multiple patients (lot 70008916, isolated from 44-year old Caucasian female; lot 2164581, isolated from 44-year old Caucasian female; lot 1917076, isolated from 40-year old Caucasian female) and T2DM–HASMCs (lot 3125, isolated from tunica media of fibrous plaques-free aorta of 49-year old type 2 diabetic Caucasian female) were purchased from American Type Culture Collection (ATCC, VA, USA), Thermo Fisher Scientific (Waltham, MA, USA), and CELL Application Inc. (San Diego, CA, USA). The cell culture medium was prepared using normal D-glucose (5 mmol/L) [24] added to Dulbecco's Modified Eagle Medium (L-DMEM) supplemented with 10% heat-inactivated fetal bovine serum (FBS), and 1% penicillin/streptomycin. All cell culture medium supplies were from Thermo Fisher Scientific.

For all the experiments, primary HASMCs and T2DM–HASMCs cells were initially passaged in T-25 culture flasks (Nunc™, Thermo Fisher Scientific) coated with 0.1% gelatin. Prior to experiments, cells were serum starved in L-DMEM (containing 1% heat-inactivated FBS, 1% pen-strep) for 24 h to synchronize cell cycles. Then, all HASMCs were exposed to varying D-glucose levels (5 mmol/L, 10 mmol/L, 20 mmol/L) [25], and T2DM–HASMCs were exposed to 5 mmol/L D-glucose levels for 21 days in 6–well plates coated with 0.1% gelatin ($n=6$ wells/ condition/ assay). To mimic diabetic conditions in vitro, VSMCs were initially cultured in normal glucose (5 mmol/L) levels for at least 72 h, before switching to high glucose (>20 mmol/L) levels for the rest of the study [26]. Cell media was replaced every 48 h, and during this time, no significant decrease in glucose concentration was noted at all the culture conditions. The glucose concentration in the medium was measured using the GlucCell™ glucose monitoring system (CESCO Bioengineering Co., Trevose, PA, USA). The final cultures were harvested and processed for biomechanical testing using AFM, transcriptomic, proteomic, and metabolic data analysis omics analysis, and cytokines/ chemokines/ growth factors quantification. Normal HASMC cultures (receiving 5 mM/L glucose) served as baseline controls, and patient-derived T2DM-SMCs served as disease controls.

Phenotype assessment

Separately, SMCs (5×10^4 cells/well) were seeded into 24-well plates and cultured under various glucose conditions for up to 7 days. At the end of each time point (days 1, 4, 7), 100 µL of MTT reagent (Sigma Aldrich) was added to each well and incubated for 1 h (37 °C, 5% CO_2). Then, 100 µL of detergent added to each well, incubated for 1 h at room temperature, and the absorbance measured at 570 nm with a BioTek Synergy H1 Hybrid multi-mode microplate reader. Wells with complete media alone and no cells were processed in similar way. The fold-change in cell density was calculated by normalizing to the readout from the initial seeding density. SMCs under various glucose conditions as well as T2DM cells were imaged at random locations using a Zeiss Axiovert A1 fluorescence microscope equipped with Hamamatsu camera and image acquisition software. At least ten images per condition were analyzed using NIH ImageJ software to quantify the perimeter and area of the cells.

Metabolomic analysis

After 21 days of culture, the medium was removed while maintaining the plates on ice, and the cell layers were sequentially washed with cold 1× PBS and cold deionized (DI) water. The cell layers were then incubated for three minutes with methanol containing 5% acetic acid at 4 °C and scraped using a cell scraper. The cell layers were pooled in a 15 mL centrifuge vial, placed on a cell rocker for 30 min in a cold room, and sonicated on ice for 15 s at 0.5 pulse rate (Branson Digital Sonifier; Marshall Scientific, Hampton, NH, USA). Metabolites were extracted by vortexing the samples for 30 s at high speed, followed by centrifugation at 17,000 ×*g* for 10 min at 4 °C. The supernatants were carefully transferred to autosampler vials and analyzed immediately by HPLC-MS untargeted conditions.

LC/QTOF analysis was performed with Agilent 6545 QTOF Mass Spectrometer coupled with Agilent 1290 Infinity II UHPLC system (Agilent Corp., Santa Clara, CA, USA). Chromatographic separation was achieved with Waters XSelect HSS T3 (2.1 mm × 100 mm, 2.1 µm) column. The mobile phase was composed of water/0.1% formic acid (A) and acetonitrile/0.1% formic acid (B). The gradient elution conditions for both positive and negative modes are as follows: 0–6 min, 5% B; 6–8 min, 35% B; 8–30 min, 90% B; 30–35 min, 5% B; 35–37 min, 5% B. Post-run equilibration time was set to 5 min, flow rate set to 0.3 mL/min, and column temperature set to 35 °C. Untargeted polar metabolomics data was acquired with Agilent MassHunter Data Acquisition software (Version B.10.1.48). Source parameters were set as follows: drying gas (N_2) temperature 300 °C and flow 11 L/min, sheath gas (N_2) temperature 350 °C and flow 11 L/min; nebulizer gas (N_2) pressure 40 psi; capillary voltage 2000 V; nozzle voltage 0 V; fragmentor voltage, 70 V; skimmer voltage, 30 V; The data obtained was processed using molecular feature extraction and time alignment using Agilent MassHunter Profinder 10.0. A 100% in at least one sample group feature presence was used to remove irreproducible features. Extracted molecular features were imported into Agilent Mass Profiler Professional (MPP) and Metaboanalyst for identification and statistical

analysis. Statistical thresholds of $p<0.05$ and fold of change (FC) > 1.5 were chosen for selecting significant molecular features. Identification of molecular features was performed utilizing both METLIN database and in-house built libraries with mass deviation < 5 ppm. Identified compounds validation was performed using internal standards and recursive analysis of pooled QC sample.

Proteomics analysis

After 21 days of culture ($n=6$ wells/ condition), cell layers were harvested on an ice platform and centrifuged at 1.5 *rcf* for five minutes at 4 °C. Cell count was done using a mini automated cell counter (ORFLO Technologies, Ketchum, ID, USA). The cell supernatant solution was discarded, and the cell pellets were processed to extract the intracellular and extracellular proteins using the Compartmental Protein Extraction Kit (Millipore Sigma) protocols recommended by the vendor. The volume for each buffer used in our study was calculated based on cell count (3.8×10^6 to 4×10^6 cells). We separated cytoplasmic (C), nuclear (N), membrane (M), cytoskeleton (CS), and extracellular matrix protein (ECM) from each well (2 independent repeats). After the extractions, the samples were homogenized, and the protein concentrations measured were between 7.17 µg and 15 µg. The samples thus obtained comprise buffers that were not suitable for direct digestion and LC-MS/MS analysis. Hence, the samples were fractionated on an SDS-page gel, each gel lane was cut into five bands, the bands were digested with trypsin, and the digests were analyzed by LC-MS/MS (Thermo Scientific Orbitrap Exploris™ 480 Vanquish Neo UHPLC). LC-MS data was searched against the human SwissProtKB database using the program Sequest. Spectral count and peptide molecular weight was used to estimate the relative abundance of proteins in these samples. More than 5400 proteins were identified in the C samples (e.g., GAPDH, actin, myosin-9, pyruvate kinase, tubulin, filamin-A, filamin-C), and over 4900 proteins were identified in the CS samples (e.g., vimentin, myosin-9, actin, pyruvate kinase PKM, filamin-C, GAPDH). The final normalized data were calculated in $\log_{10}$-fold change to determine the magnitude of change in protein abundance between the experimental groups. Such changes were used to identify up- and down- regulation of genes. Furthermore, pathway enrichment analysis for differentially expressed genes using ReactomePA [27] enabled identification of biological pathways that are differentially regulated.

Cytokine/ chemokine/ growth factors analysis

The cytokines, chemokines and growth factors released in HASMC and T2DM–SMCs cultures were quantified using Discovery Assays® (Eve Technologies, Alberta, Canada) as we detailed earlier [28]. Briefly, the pooled spent media from each culture condition at day 21 were processed using Human Cytokine/ Chemokine 71-Plex Discovery Assay® Array (sensitivity: 0.5–10 pg/mL) and Human MMP & TIMP Panel assay (sensitivity: 0.5–14 pg/mL). Analytes were quantified using multiplex LASER bead technology and bead analyzer (Bio-Plex 200), where antibody-conjugated fluorophore beads simultaneously detect multiple analytes from a single assay.

RNA isolation and sequencing

RNA was extracted from cultured HASMCs and T2DM–HASMCs using Trizol RNA isolation reagent protocol (Thermo Fisher Scientific). Briefly, cell layers were washed with cold 1× PBS, and 1 mL of Trizol reagent was added to each well, and cells were harvested using a cell scraper. Cells were homogenized using a sonicator (Branson Digital Sonifier) and incubated at room temperature for five minutes. A 200 µL aliquot of chloroform was added to the cell supernatant and the colorless aqueous phase containing RNA was separated carefully without disturbing interphase. To ensure that each library meets the required standards for sequencing, the library quantity and quality are evaluated using Tapestation and Qubit. Tapestation (Agilent 4200 Tapestation System) high-throughput quality control device was used for RNA fragment analysis and a 2100 Agilent Bioanalyzer was used for checking RNA integrity number (RIN) score (that ranged from 9.6 – 9.8). Further, a Qubit Fluorometer (Invitrogen) was used to measure accurate concentration of RNA samples. All the samples were pooled, and molarity for sequencing is determined via qPCR (QuantaBio Q qPCR). Finally, the pooled libraries were sequenced using Novaseq 6000 platform with Illumina's sequencing reagents. Data processing and quality control checks were performed on raw fastq files. Subsequently, the readings were aligned with bowtie2 and quantified using RSEM (RNA-Seq by Expectation-Maximization). Differential expression analysis was conducted on mapped read counts obtained from RSEM using the R/Bioconductor package EBSeq. The analysis identified upregulated and downregulated genes, which were then used for Gene Set Enrichment Analysis and Venn diagram plotting.

Confocal microscopy

HASMCs under three different conditions mimicking healthy, prediabetic and diabetic conditions, and T2DM–HASMCs were cultured for 21 days in multi-chamber cell culture slides (Thermo Fisher Scientific). The cell culture medium was discarded, and cells were washed with 1× PBS, fixed with 4% paraformaldehyde for 30 min, permeabilized with 0.1% Triton X-100 in PBS for 5 min, and blocked with 2% bovine serum albumin (BSA) for 30 min. The cells were washed with 1× PBS and incubated with

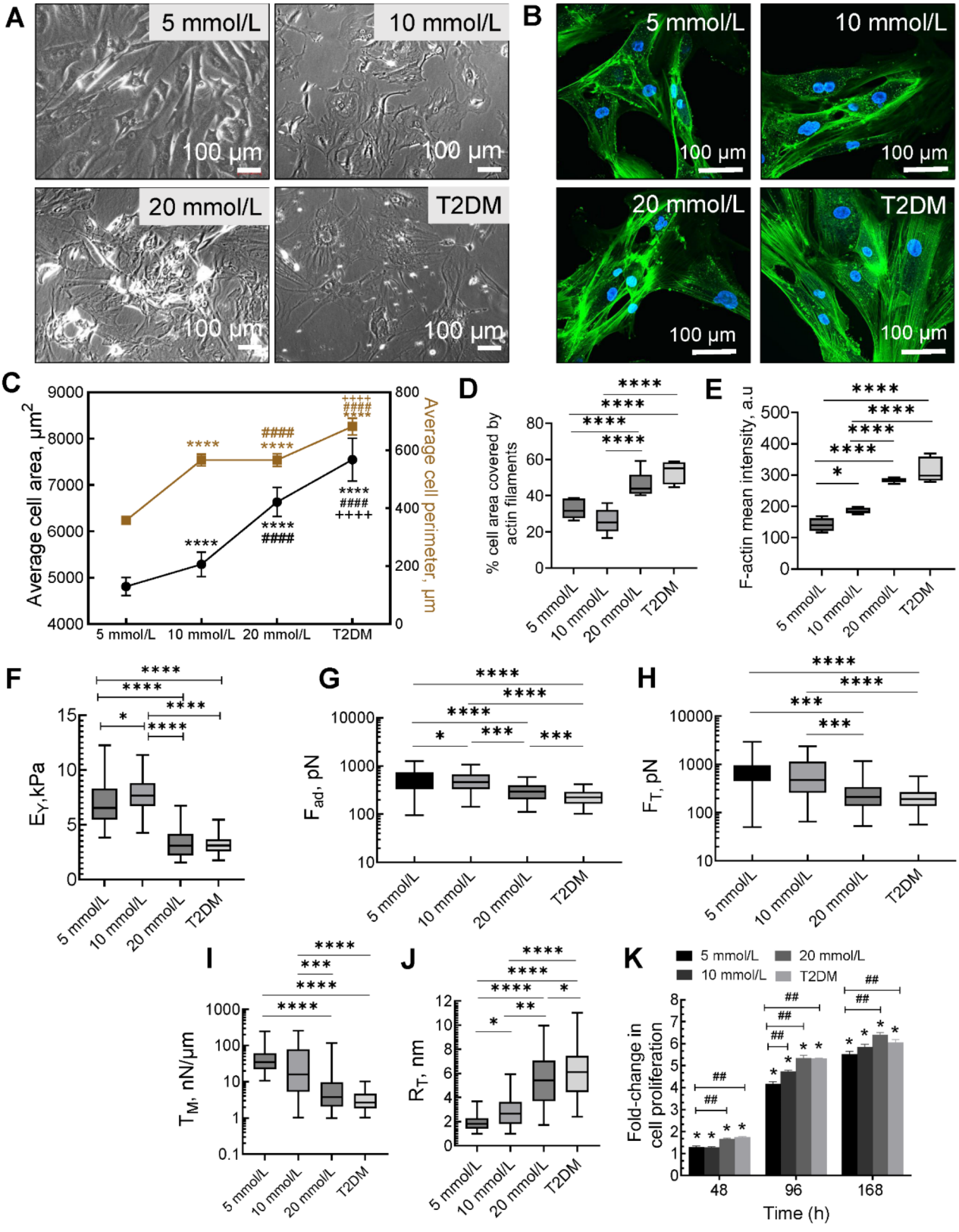

Fig. 1 (See legend on next page.)

(See figure on previous page.)

Fig. 1 **A**. Representative phase-contrast images of adult human aortic SMCs cultured under varying glucose concentrations (5, 10, or 20 mmol/L), and T2DM SMCs. **B**. Representative confocal images of filamentous-actin (F-actin) and nuclei (blue) stained with Alexa Fluro 488-phalloidin and DAPI, respectively. **C**. Significant differences in average cell area and perimeter were noted between SMCs treated with various dosages of glucose and with T2DM SMCs. Data shown represents mean ± standard error in respective cases ($n > 50$ cells/condition). **** indicates $p < 0.0001$ vs. 5 mmol/L cultures; #### indicates $p < 0.0001$ vs. 10 mmol/L cultures; ++++ indicates $p < 0.0001$ vs. 20 mmol/L cultures. **D**. Quantitative analysis of area occupied by F-actin within SMCs exposed to various culture conditions. **E**. Quantitative analysis of fluorescence intensity of F-actin. Analysis of fluorescence intensity was done at the original magnification by measuring the mean gray value with Fiji ImageJ software. Data was pooled from $n = 6$ wells/ condition for each of these assays. Biomechanical characteristics such as elastic modulus (E_Y, **F**), forces of adhesion (F_{ad}, **G**), membrane tether forces (F_T, **H**), membrane tension (T_M, **I**), and tether radius (R_T, **J**) were quantified from the AFM data. E_Y data were calculated by applying Hertz model to force–indentation curves ($n \geq 100$ cells/condition) obtained from cells. F_{ad} and F_T were measured by retraction of beaded-AFM probe from the cell surface. In plots D-J, the center line in the box plots denotes the median, and bound of box shows 25th to 75th percentiles, while upper and lower bounds of whiskers represent the maximum and minimum values, respectively. * indicates $p < 0.05$, ** indicates $p < 0.01$, *** indicates $p < 0.001$, and **** indicates $p < 0.0001$. **K**. Proliferation of human SCMs under various glucose conditions as well as that of T2DM-SMCs. * indicates $p < 0.05$ vs. initial cell seeding density, ## indicates $p < 0.01$ for control (5 mmol/L) vs. glucose treatment (10 mmol/L, 20 mmol/L; T2DM)

phalloidin-iFluro 488 (Abcam) and 4′,6-diamidino-2-phenylindole (DAPI, Sigma), at room temperature for 90 min, to stain for F-actin and nuclei, respectively. Cells were washed with 1× PBS to remove excess staining solution and imaged using a Nikon A1Rsi confocal laser scanning microscopy. To quantify actin expression in SMCs exposed to varying glucose levels, images were captured with a 40× objective, transformed into grayscale images, and mean fluorescence intensity of actin filaments analyzed using Fiji ImageJ software. Three independent experiments were performed. Several fields of view of equal size per glucose treatment were randomly selected and mean fluorescence intensity of actin expression were measured and compared to controls.

Atomic force microscopy

HASMCs were cultured for 7 days in 60–mm gelation-coated petri dishes under various glucose concentrations, while T2DM–HASMCs were cultured under normal glucose conditions. Cells were maintained at 37 °C for live-cell nanoindentation performed using an MFP-3D-Bio AFM (Asylum Research, Oxford Instruments, Santa Barbara, CA) mounted on an inverted optical microscope (Nikon Eclipse Ti). Tip-less AFM cantilevers (Nano World, Arrow TL 1, nominal spring constant ~ 0.03 N/m) were modified by attaching a 5-µm polystyrene bead using epoxy. The actual spring constant was determined using the thermal calibration method in a clean culture dish before each experiment and thermal/mechanical equilibrium of AFM was achieved by submerging probe in cell medium for stabilization. For each condition, at least 50 cells were randomly chosen and intended at random locations at 0.3 Hz with constant trigger point of 0.3 V. Force-indentation curves were obtained and Young's modulus (E_Y) was determined from these curves using Hertz's contact model. The force of adhesion (F_{ad}) and tether forces (F_T) were obtained from the force-indentation curves, from which membrane tension ($T_M = F_T^2/8\pi\,^2 K_B$) and tether radius ($R_T = 2\pi\, K_B/F_T$) were calculated [29]. Frequency distribution and one-way ANOVA were performed for statistical analysis and $p < 0.05$ was considered significant.

RNA-seq data analysis

RNA-seq reads were mapped to the human reference genome (version: GRCh38) and corresponding annotated protein-coding genes using Bowtie [30], allowing up to 2-mismatches. The gene expected read counts and Transcripts Per Million (TPM) were estimated by RSEM [31]. The TPMs were further normalized by EBSeq [32] R package to correct the potential batch effect. The EBSeq package [32] was further used to assess the probability of gene expression (mRNAs) being differentially expressed between any two given conditions. We required that DEGs should have FDR < 5% via EBSeq and > 2 fold-change of "median-by-ratio normalized read counts + 1".

Pathway enrichment analysis

The Reactome pathway enrichment analysis was performed by the "ReactomePA" R package [33].

Statistical analysis

To evaluate the changes in SMC phenotype, metabolomics, proteomics, and RNA-seq, at least $n = 6$ wells/ condition/ cell type/ assay were cultured. The spent media from these wells were pooled and processed for cytokine/ chemokine/ growth factor analysis. For AFM analysis, at least 50 cells from each condition were analyzed. Data from human SMCs and T2DM SMCs were pooled and expressed as scatter plots with mean ± SEM where appropriate. Descriptive statistical analyses were conducted using the GraphPad Prism 10 software. A one-way ANOVA with post hoc Tukey's test was used for multiple comparisons of the results from various assays, with statistical significance set at $p < 0.05$.

Results and discussion

Hyperglycemic conditions induce phenotypic changes in human aortic SMCs

Significant differences in morphology and phenotype were evident in SMCs exposed to various glucose

conditions (Fig. 1, A, B). It was noted that cells were more aggregated, irregular in shape, and larger in cross-sectional area within high glucose cultures, contrasting with the regular and standalone appearance in 5 mmol/L cultures. T2DM cells lacked the hill and valley configuration seen in normal SMCs, in line with that reported by others [34]. Analysis of the cell morphologies from multiple such images revealed that the cell area and perimeter significantly increased at higher glucose concentration (Fig. 1, C; $p<0.05$), whereas T2DM cells were the largest in size ($p<0.05$) among all the cases. This is to be expected because high glucose levels reportedly have differential effects on the phenotype and function of many cell types. The cell morphology was analyzed using the cell shape index, i.e., $CSI = 4\pi A/P^2$, where A and P are the measured cell area and perimeter, respectively [35]. Results indicated that SMCs exposed to 10 mmol/L and 20 mmol/L glucose had *CSI* around 0.23 ± 0.01, whereas T2DM cells and normal SMCs (5 mmol/L) had CSI around 0.48 ± 0.03 ($p < 0.001$). It should be noted that the area and perimeter of the SMCs in control (5 mmol/L glucose) cultures is in broad agreement with literature [36]. Quantitative analysis revealed elevated levels of F-actin expression in SMCs receiving higher glucose concentrations (Fig. 1, D, E). The area covered by actin within the cells as well as the fluorescence intensity of actin were significantly higher in 20 mmol/L glucose treated cells and T2DM-SMCs compared to cells receiving 5 mmol/L or 10 mmol/L glucose ($p<0.05$). Collectively, these results suggest that exposure of VSMCs to elevated glucose levels for longer periods induces significant phenotypic changes in these cells, broadly comparable to their T2DM counterparts.

The Young's modulus (E_Y) of SMCs in normal glucose conditions (5 mmol/L) was noted as 7.03±2.01 kPa (Fig. 1, F). While 10 mmol/L glucose did not contribute to significant changes in E_Y (7.78±1.65 kPa; $p>0.05$ vs. 5 mmol/L), 20 mmol/L glucose significantly reduced E_Y to 3.32±1.3 kPa ($p<0.05$ vs. 5 mmol/L; $p<0.05$ vs. 10 mmol/L glucose). T2DM cells exhibited E_Y (3.19±0.84 kPa) similar to SMCs that received 20 mmol/L ($p<0.01$ vs. 5 mmol/L; $p<0.01$ vs. 20 mmol/L). The E_Y of SMCs in 5 mmol/L glucose conditions was similar to our previous study [37], whereas the E_Y of T2DM-SMCs is in close range to values reported in literature [38]. Human coronary SMCs derived from healthy patients reportedly had higher E_Y than those isolated from T2DM patients [38], in agreement with our results here. However, in coronary vascular SMC cultures, isolated from control or diabetic mice, no significant impact of glucose concentration on E_Y was reported [38]. SMCs receiving 5 mmol/L glucose recorded adhesion forces (F_{ad}) of 558±229 pN (Fig. 1, G), and increasing the glucose concentration significantly decreased these adhesion forces ($p<0.05$ vs. 5 mmol/L; $p<0.05$ for 10 mmol/L vs. 20 mmol/L). T2DM cells had the lowest adhesion forces of all the cases tested (233±71 pN; $p<0.05$ vs. all other cases). The tether forces (F_T) recorded in SMCs cultured with 5 mmol/L glucose was 787±342 pN (Fig. 1, H), and while 10 mmol/L glucose had no effect on these values, 20 mmol/L significantly reduced the F_T (286±109 pN; $p<0.05$ vs. 5 mmol/L and 10 mmol/L). T2DM cells recorded the lowest F_T among all the test cases and was not significantly different from 20 mmol/L condition.

The force needed to deform a cell membrane, also termed as the apparent membrane tension (T_M), was calculated from tether forces using $T_M \cong F_T^2/8\pi^2 K_B$, where K_B is the bending stiffness that lies in the 0.1–0.3 pN.μm range [39, 40]. The T_M values were as follows (Fig. 1, I): 5 mmol/L (50.4±2.3 nN/μm), 10 mmol/L (53.7±3.2 nN/μm), 20 mmol/L (11.4±0.9 nN/μm), and T2DM (3.5±0.2 nN/μm). The T_M was significantly lower in cells receiving 20 mmol/L glucose versus other glucose concentrations ($p<0.01$), and T2DM cells have the lowest T_M of all the cases tested ($p<0.01$). The tether radius (R_T) increased with increasing glucose concentration (Fig. I, J), with control (5 mmol/L) cells having 1.9±0.03 nm on average and T2DM cells having 6.1±0.13 nm. To the best of our knowledge, the F_T, F_{ad}, T_M and R_T values for human SMCs and specifically under diabetic conditions haven't been reported earlier in literature.

Previously, we reported that primary SMCs derived from human aneurysmal aortae and analyzed using AFM exhibited the following values [41]: E_Y = 20.9±7.7 kPa, F_{ad} = 1.87±0.13 nN, F_T = 218.8±14.3 pN, T_M = 6.07±0.8 nN/μm, and R_T = 2.91±0.19 nm. Compared to T2DM SMCs and SMCs receiving higher glucose in the current study, it is evident that human aneurysmal aortic SMCs (yet another CVD condition) have significantly higher E_Y, F_{ad} and R_T ($p<0.01$ in all the cases), although the tether forces and membrane tension of T2DM SMCs were comparable to that in aneurysmal SMCs, underlying the differences in the pathologies of these two vascular diseases.

Compared to SMCs cultured for 24 h, cell proliferation increased 1.3–1.75 –fold after 48 h, 4.1–5.35 –fold after 96 h, and 5.5–6.1 –fold after 7 days (Fig. 1, K) in all the cases. Cell proliferation increased with time at each glucose concentration, as well as in T2DM cultures. Our findings are consistent with previous reports where high glucose led to significant increase in the proliferation of various cell types compared to normal glucose levels [42]. For instance, previous studies reported a 3–fold increase in VSMC proliferation exposed to high glucose (>20 mmol/L) compared to controls (5 mmol/L), as measured using the MTT assay [43–45].

Hyperglycemia has been linked to numerous facets of arterial modeling. Elevated glucose levels have been shown to alter trophoblast proliferation and invasion,

thereby contributing to SMC mediated arterial remodeling during fetal growth and development [46]. T2DM patients with higher glucose levels had larger common carotid artery intima-media thickness, luminal diameter, and brachial pulse pressure compared to their healthy counterparts, suggesting adaptive remodeling of stiffened arteries [47]. Clinically, T2DM has been implicated in remodeling of calcified arteries that exhibit significantly greater necrotic cores and inflammation, primarily driven by macrophages and lymphocytes [48]. Hyperglycemia induces significant changes in vascular ECM composition and remodeling capabilities, ultimately leading to compromised vessel function and stiffer vessel walls [49]. A majority of these changes are driven by alternations in SMC phenotype, function, and mechanobiology, resulting in diseases such as stroke, aneurysm, and hypertensive vessels [16, 50].

Differential effects of hyperglycemia on cytokine/ chemokine/ growth factor release by SMCs

The release of cytokines and chemokines in chronic SMC cultures were quantified (Fig. 2) and significant variations in analyte concentrations depending on glucose concentration were noted. Some interleukins that weren't expressed at all or released in extremely low levels by T2DM cells (e.g., IL-9, IL-17 A, IL-17 F, IL-28 A, IL-4, IL-15, IL-25, IL-33) were seen in SMC cultures receiving glucose (Fig. 2, A). On the other hand, interleukins such as IL-6, IL-8, IL-23 and IL-27 were released in higher levels in T2DM cells than in SMCs receiving glucose. Among various cytokines and chemokines tested (Fig. 2, B), higher levels of SCD40L, RANTES, GROα, MCP-1, M-CSF, and MIP-1δ were noted in T2DM cultures than in SMC cultures receiving glucose. On the other hand, G-CSF was higher in SMC cultures receiving glucose than in T2DM cultures. There weren't any significant differences in the expression of other cytokines and chemokines between the various culture conditions. T2DM has been linked to immune system disorders as well as elevated levels of IL-6, IL-18, MCP-1, and TNF-α [51–53]. Although TNF-α, IL-18, and IFN-γ levels were similar in all the cases we tested, IL-6 and MCP-1 levels were significantly higher in T2DM cells consistent with literature.

FGF-2 levels were slightly higher in SMC cultures receiving 5 and 10 mmol/L glucose, whereas TGF-β2 and TGF-β3 levels were significantly lower in T2DM cultures

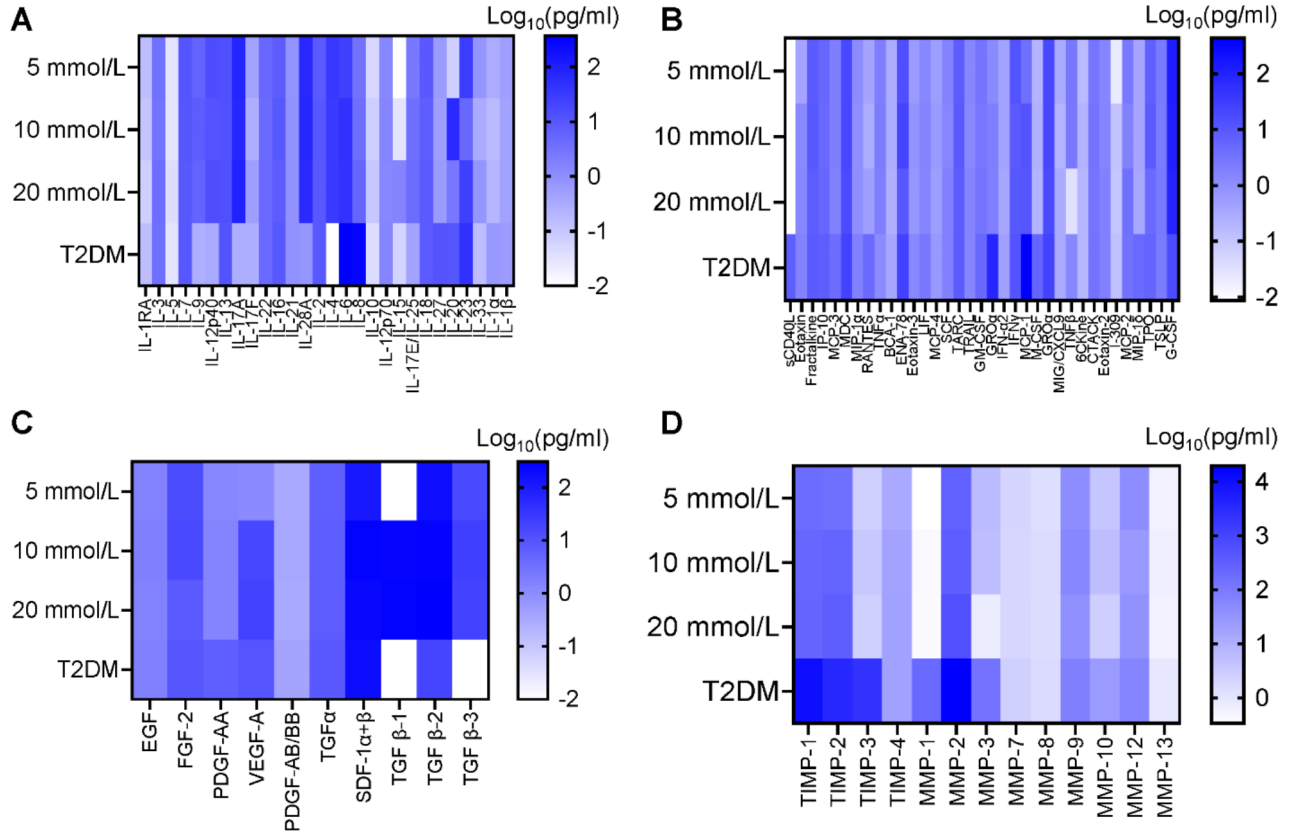

Fig. 2 Heat maps of the levels of interleukins (**A**), cytokines & chemokines (**B**), growth factors (**C**), and MMPs/TIMPs (**D**) released in SMC cultures receiving various glucose concentrations and from T2DM cells over 21 days. Spent media was pooled from at least $n = 6$ wells/ condition and processed to measure the levels of these markers

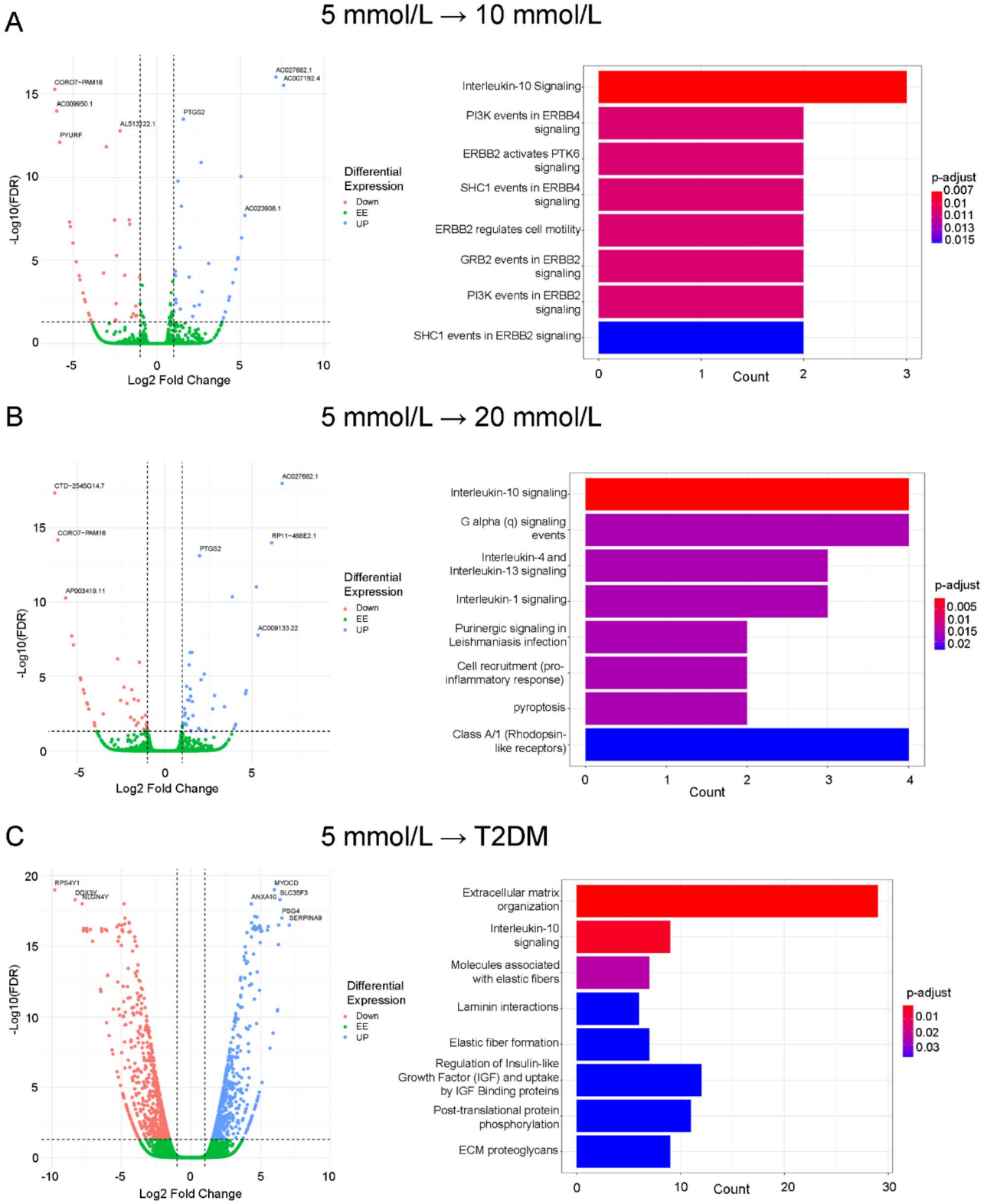

Fig. 3 Volcano plots of differential gene expression patterns and enriched pathways in response to glucose concentration and diabetic conditions. (**A**) 10 mmol/L vs. 5 mmol/L glucose, (**B**) 20 mmol/L vs. 5 mmol/L glucose, and (**C**) T2DM Vs 5 mmol/L glucose. Cell pellets were pooled from $n=6$ wells/condition for RNA-seq analysis

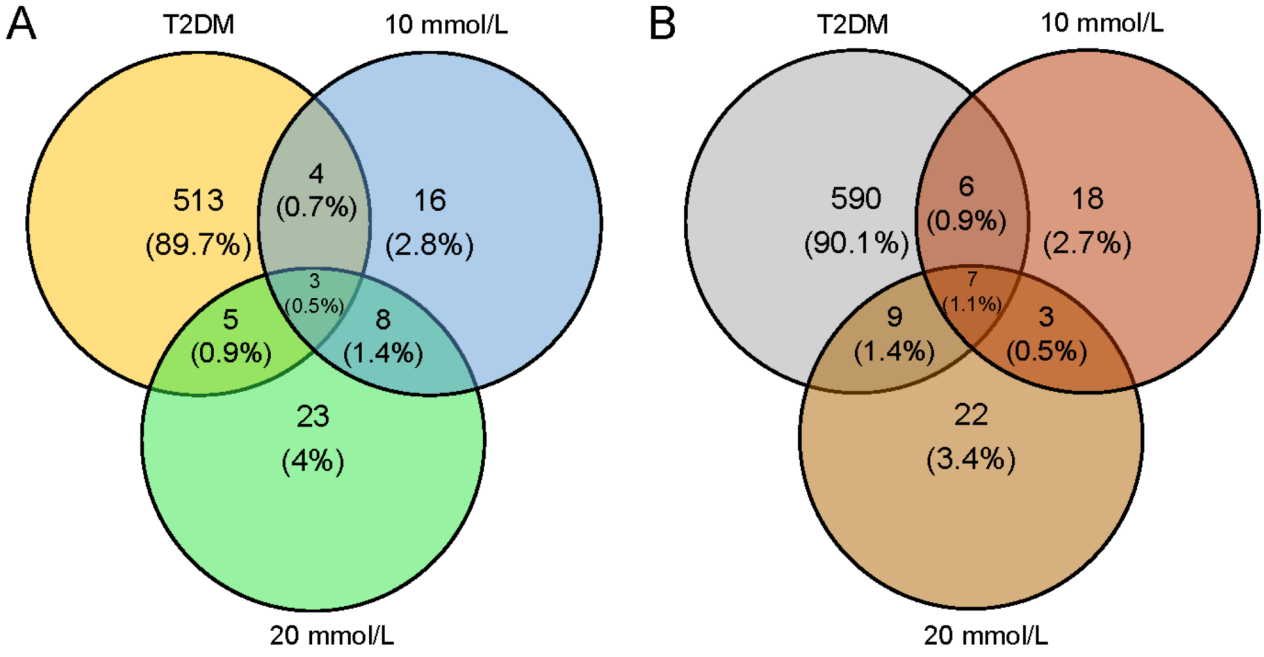

Fig. 4 Venn diagram indicating the overlap between differentially expression genes (DEG) in SMCs receiving various glucose concentrations (10 mmol/L and 20 mmol/L). RNA-seq data for each condition was compared to cells receiving 5 mmol/L glucose. T2DM cells were also shown for comparison. (**A**) Up-regulated differentially expressed genes; (**B**) down-regulated differentially expressed genes. Cell pellets were pooled from $n=6$ wells/ condition for RNA-seq analysis

(Fig. 2, C). The levels of VEGF-A, PDGF-AA, and TGF-β1 were higher in cultures receiving 10 and 20 mmol/L glucose. Similar to our observation, high glucose (20 mmol/L) was shown to elevate TGF-β1 and TGF-β-R1 receptor expression in vascular SMCs, via protein kinase C (PKC-α) activation [54]. Hyperglycemia was shown to induce VEGF-A expression in SMCs similar to acute insulin treatment [55], with implications in decreased function and failure of multiple organs (e.g., retina, kidneys). Our study showed that VEGF-A levels were significantly elevated (>40-fold; $p<0.001$ vs. 5 mmol/L) in the presence of 10 mmol/L and 20 mmol/L glucose to levels noted in T2DM cells.

MMPs–1, 2, 3 and TIMPs–1, 2, 3 were elevated in T2DM cells than glucose-receiving HASMC cultures (Fig. 2, D). These results suggest that SMCs treated with varying glucose concentrations directly influence the expression of various cytokines, chemokines, growth factors and MMPs/ TIMPs. High glucose exposure was shown to increase transcription and translation of MMPs–1, 2, 9 and 13 in human SMC cultures and their enzymatic activity, especially in the presence of macrophages, representative of T2DM conditions in vivo [56]. Consistent with this report, we here note that these specific MMPs were significantly higher in T2DM cultures, whereas MMPs–2, 9 and 12 were also present in SMC cultures receiving high glucose levels. The interplay between MMPs and TIMPs regulate the development of atherosclerotic plaques and arterial remodeling under diabetic conditions [57]. In humans with T2DM and hypertension, elevated levels of TIMPs-1 and 3, TIMP-1: MMP-2 ratio, and TIMP-1: MMP-9 ratio were reported [58, 59], which mirrors our observations in this study.

It is worth noting that previous studies suggest that when human aortic SMCs were co-cultured with macrophages under normal (5.5 mmol/L) and high glucose (25 mmol/L) conditions, SMCs exhibited augmented gene and protein expression of MMP-1 and MMP-9, significant increase in MMP-9 enzymatic activity, higher levels of soluble and functionally-active MCP-1 linked to MMPs upregulation, and activated PKCα signaling pathway that together with NF-kB is responsible for MMPs-1, 9 upregulation [56].

Inflammatory cytokines-associated pathways are enriched in hyperglycemia induced upregulated genes

Previous research has independently analyzed the transcriptome, proteomics, and metabolomics to identify distinct markers in diabetic SMCs [60]. Our current study, however, profiles these as paired omics data. We explored which genes correspond with metabolomics profiling patterns and the implications of these correlations within

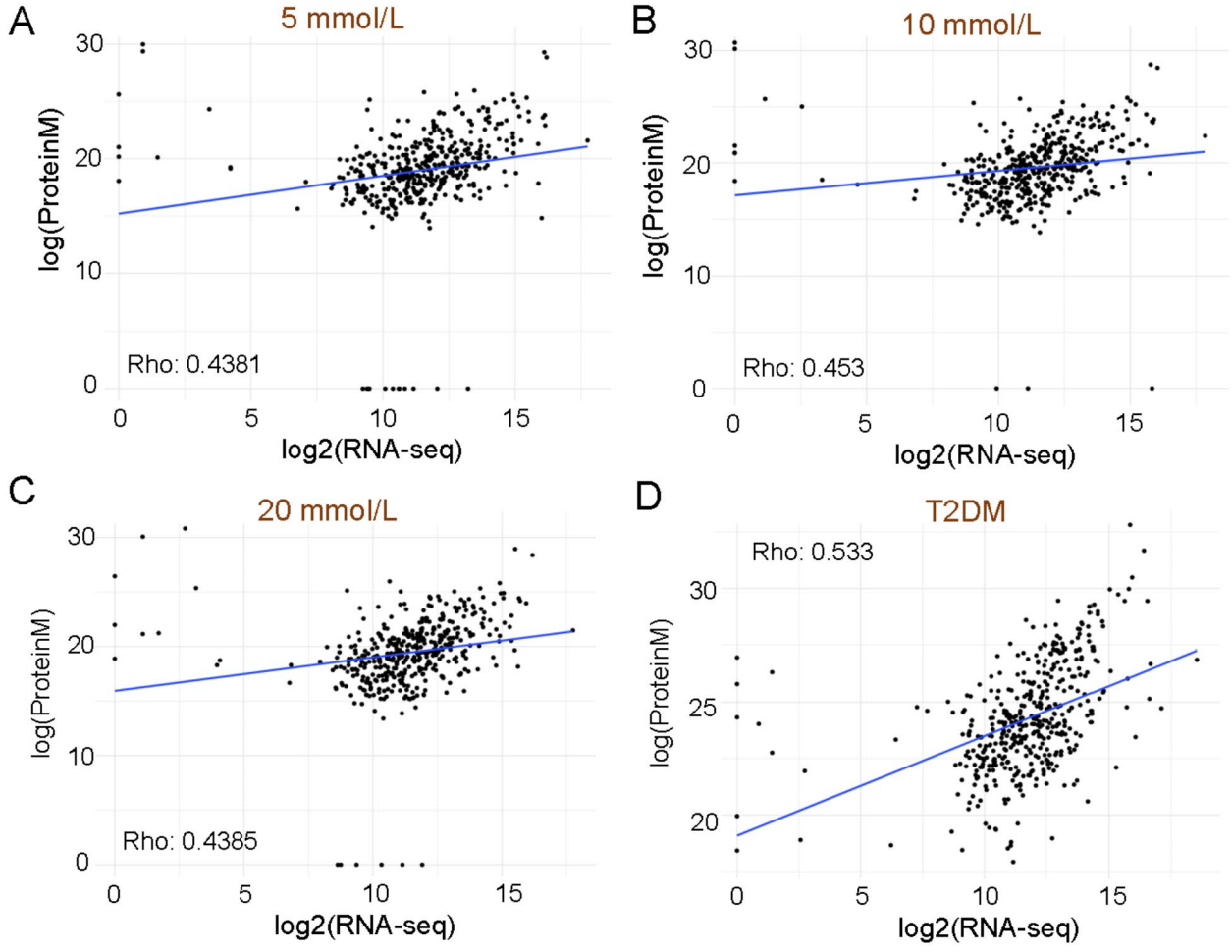

Fig. 5 Correlation between ECM proteins and mRNA levels across various glucose conditions and T2DM patient samples for 448 genes. (**A**) 5 mmol/L: Spearman correlation coefficient of 0.438 ($p = 1.67 \times 10^{-21}$). (**B**) 10 mmol/L: Spearman correlation coefficient of 0.453 ($p = 4.11 \times 10^{-23}$). (**C**) 20 mmol/L: Spearman correlation coefficient of 0.439 ($p = 1.53 \times 10^{-21}$). (**D**) T2DM: Spearman correlation coefficient of 0.533 ($p = 7.55 \times 10^{-33}$). Cell pellets were pooled from $n = 6$ wells/ condition for RNA-seq and proteomic analysis

the omics modules. We also examined how mRNA levels align with protein abundance. This integrated dataset analysis deepens our understanding of chronic hyperglycemia-induced changes in human aortic smooth muscle cells, advancing beyond mere biomarkers to explore their complex relationships.

We first investigated the genes upregulated by hyperglycemia enriched pathways. Vascular SMCs receiving 5 mmol/L glucose were compared to those receiving 10 mmol/L (Fig. 3, A) or 20 mmol/L (Fig. 3, B) glucose, and T2DM-SMCs (Fig. 3, C). Pathway enrichment analysis was further performed by the differentially expressed genes (DEGs). We found that inflammatory cytokine-associated pathways, especially those involving IL-10 signaling, are prominently enriched in genes that are upregulated by increased glucose levels of 10 mmol/L and 20 mmol/L glucose, compared to normal glucose levels. IL-10 signaling pathway has been shown to modulate the function of various immune cells. Studies have shown that elevated IL-10 pathways are associated with multiple autoimmune diseases [35]. Additionally, we observed that genes activated by a higher glucose concentration of 20 mmol/L are more closely associated with inflammatory cytokine pathways, including not only IL–10 but also ILs – 1, 4 and 13 signaling pathways (Fig. 3, B). This aligns with the hypothesis that long-term exposure to high glucose levels leads to enhanced inflammatory responses, which are associated with chorionic inflammation. The genes involved in the activation of G-alpha signaling events were significantly enriched in SMCs receiving 20 mmol/L glucose but not in SMCs supplied with 10 mmol/L glucose. G-alpha is involved in the inhibition of cAMP dependent pathway which in turn leads to reduced activity of cAMP-dependent protein kinases, as well as activation of the protein tyrosine kinase c-Src [61, 62].

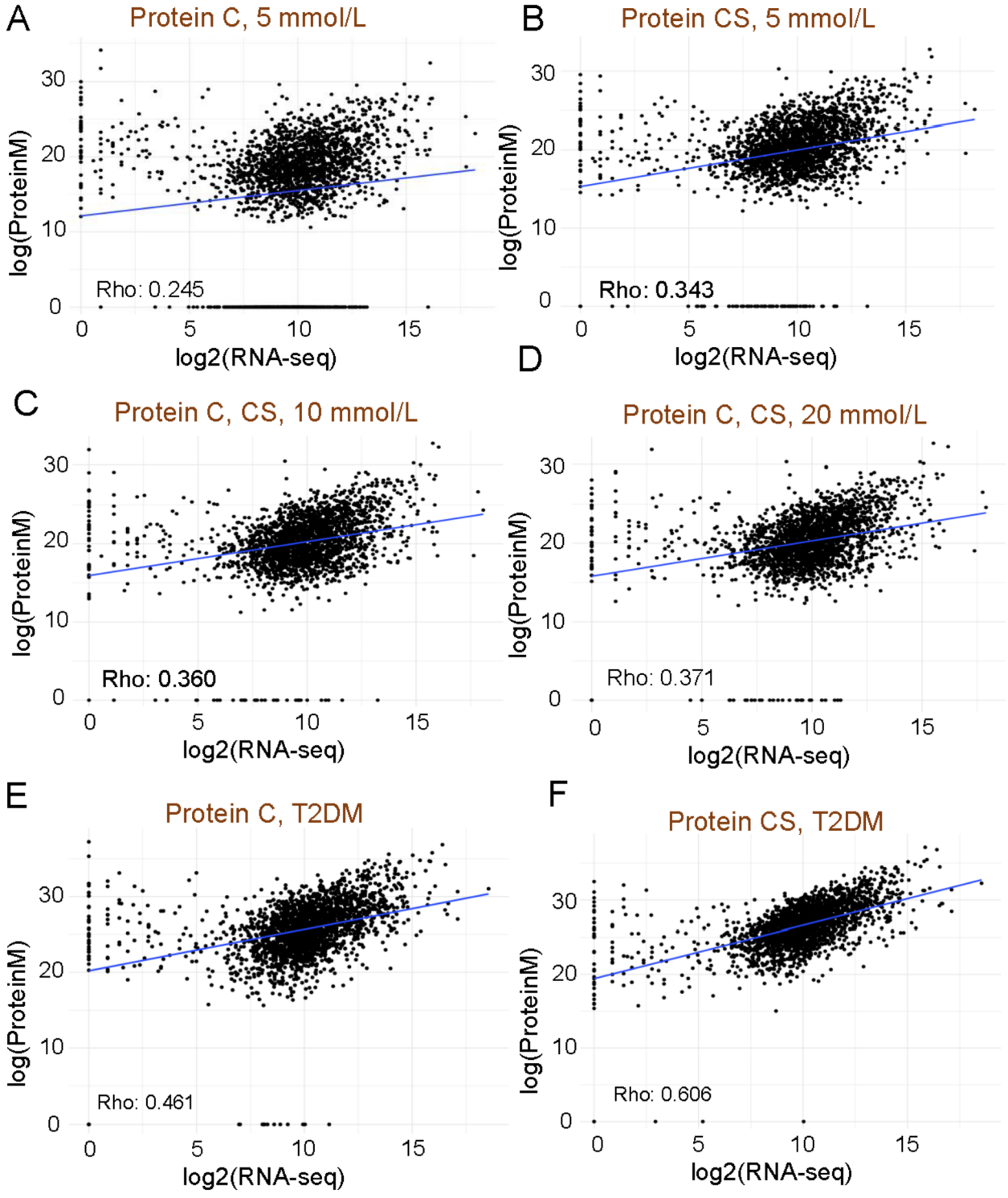

Fig. 6 The correlation between mRNA expression levels and cytosol (C) / cytoskeletal (CS) protein levels for 2323 genes across different culture conditions. (**A**) 5 mmol/L glucose: Spearman correlation coefficient of 0.245 ($p = 2.67 \times 10^{-33}$) for cytosol protein. (**B**) 5 mmol/L condition: Spearman correlation coefficient of 0.343 ($p = 3.71 \times 10^{-65}$) for cytoskeleton protein. (**C**) 10 mmol/L: Spearman correlation coefficient of 0.363 ($p = 2.61 \times 10^{-72}$) for both cytosol (C) and cytoskeleton (CS) protein. (**D**) 20 mmol/L: Spearman correlation coefficient of 0.371 ($p = 7.58 \times 10^{-77}$) for both cytosol (C) and cytoskeleton (CS) protein. (**E**) T2DM: Spearman correlation coefficient of 0.461 ($p = 1.19 \times 10^{-122}$) for cytosol protein. (**F**) T2DM patient samples: Spearman correlation coefficient of 0.606 ($p = 7.57 \times 10^{-234}$) for cytoskeleton protein. Cell pellets were pooled from $n = 6$ wells/ condition for RNA-seq and proteomic analysis

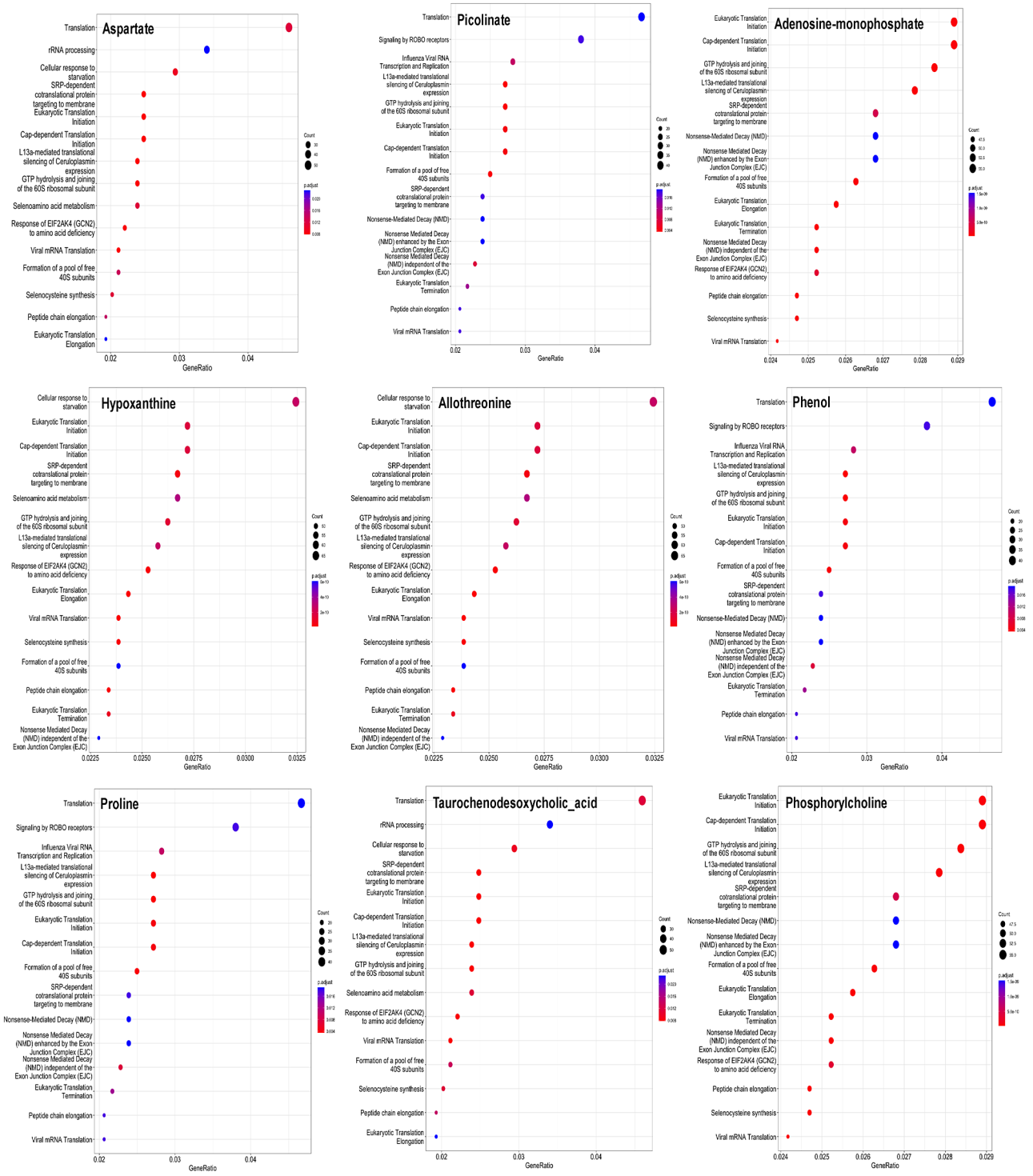

Fig. 7 Nine enriched pathways from co-expression analysis associated with compounds involving L13a-mediated translational silencing of ceruloplasmin expression: aspartate, picolinate, adenosine-monophosphate, hypoxanthine, allothreonine, phenol, proline, taurocheno-desoxycholic acid, and phosphorylcholine. Cell pellets were pooled from $n = 6$ wells/ condition for metabolomic analysis

The epidermal growth factor receptor family (EGFR or ErbB 1–4) has been implicated in various cellular functions (e.g., growth, division, differentiation, migration, apoptosis) and multiple downstream signaling pathways (e.g., ERK1/2, MAP, PI3-kinase/Akt) under hyperglycemia or diabetes (types I and II) conditions and related cardiovascular outcomes [63]. In our study, compared to normal glucose levels, chronic exposure to 10 mmol/L

but not 20 mmol/L glucose appears to have resulted in differentially expressed genes related to ErbB2 and ErbB4 and their functions and pathways (cell motility, PI3K, PTK6, SHC1) in human vascular SMCs.

We found a notable distinction between the gene expression patterns in cells exposed to high glucose levels in vitro (10 or 20 mmol/L) and those compared to T2DM-SMCs (Fig. 3, C). Despite some similarities, the up-regulated genes in T2DM cells did not entirely correspond with those observed in the high glucose in vitro models. This could possibly be due to the multifactorial nature of T2DM in vivo and exposure of SMCs to chronically (multi-year) elevated levels of high glucose and inflammatory molecules under such conditions. In T2DM-SMCs, the dominant pathways involved relate to ECM organization (e.g., laminin, elastin, collagens, proteoglycans, GAGs) and the regulation of IGF, highlighting the complexity of diabetes pathogenesis beyond the changes induced by hyperglycemia alone. This is to be partially expected because T2DM diagnosis could also be an indicator of the onset of various proteolytic vascular conditions such as atherosclerosis that results in arterial remodeling and SMC activation, which is reflected in the cells isolated from a T2DM tissue. Interestingly, IL-10 pathways were enriched in both the in vitro models and in T2DM-SMCs, suggesting that increased inflammatory cytokine-associated pathways are a consistent feature of prolonged hyperglycemia. This could potentially contribute to the pathogenesis of diabetic complications, particularly in vascular tissues, implying that controlling inflammation may be crucial in preventing these complications. Interestingly, compared to SMCs receiving normal glucose levels, T2DM cells had altered gene expression for molecules involved in ECM organization, elastic fiber synthesis and formation, laminin interactions, and ECM proteoglycans, highlighting the role of T2DM in arterial remodeling.

Similar outcomes were noted from the differentially regulated gene (DGE) analysis (Fig. 4) performed on these cells. We performed statistical analysis on the normalized read count data to assess quantitative changes in expression levels between the various groups. Compared to SMCs receiving normal glucose levels, 513 genes were upregulated, and 590 genes were downregulated in T2DM cells (list of genes provided in Table S1). We note that, among others, the genes involved in arterial remodeling were significantly upregulated in T2DM cells (e.g., COL, ELN, GLB, FBLN, LMN). We performed a ReactomePA analysis to identify the pathways enriched for the upregulated and downregulated genes, respectively). Cells receiving 10 and 20 mmol/L glucose have much fewer genes that were differentially expressed, while very few of these genes were common between all the cell types.

In the medial layers of healthy vascular ECM, circumferential layers of collagens, elastic fiber associated proteins (elastin, fibrillin, fibulins, microfibril-associated glycoproteins), as well as basement membrane proteins (collagen type IV, laminins, fibronectin) are present [64]. The signaling from healthy collagens and elastic fibers maintain vascular SMCs in a quiescent, differentiated state and contributes to normal SMC functions. Vascular injuries and diseases such as T2DM induce changes in the tissue ECM (e.g., proteolysis of ECM proteins) and activates and dedifferentiates SMCs to a more proliferative and invasive phenotype, disturbing the ECM protein-SMC signaling pathways [49]. Hyperglycemic conditions were shown to increase osteogenic genes expression in vascular SMCs, and enhance the stiffness of arterial elastin and glycation of elastic fibers, leading to arterial calcification associated with diabetes [65]. Others reported that hyperglycemia and T2DM conditions significantly alter the expression of ECM genes such as elastin, fibulin, laminin, and collagen [66–69], which in turn contribute to undesirable outcomes in arterial remodeling. Our results indicate upregulation of COL, ELN, GLB, FBLN, LMN genes in T2DM cells, highlighting their role in disease pathogenesis and arterial remodeling. Upregulation of these genes could lead to significant increases in their protein synthesis and deposition, which contributes to ECM remodeling, cell-ECM interactions, and cell migration.

Using a microarray dataset (GSE26168) from the Gene Expression Omnibus database, Zhu et al.. identified 981 DEGs, of which 301 were upregulated and the rest downregulated [70]. These DEGs were highly enriched in cell differentiation, cell adhesion, intracellular signal transduction, and regulation of protein kinase activity, as well as cAMP signaling pathway, Rap1 signaling pathway, regulation of lipolysis in adipocytes, PI3K-Akt signaling pathway, and MAPK signaling pathway. Based on the PPI network of these DEGs, the top 6 genes contributing to T2DM initiation, progression, and intervention strategy were identified as PIK3R1, RAC1, GNG3, GNAI1, CDC42, and ITGB1. While none of these specific genes were in measurable levels in our cultures, GNG2, CDC20, CDCP1, and ITGB8 were upregulated, whereas PIK3IP1 and ITGB3 were downregulated in T2DM cells. However, despite differences in the individual gene signatures between the two datasets and the underlying approaches (microarray in their study vs. RNA-seq here), pathway analysis highlights broad consistencies between our data and that reported by Zhu et al.

Significant correlations between mRNA and protein expression levels

We conducted a comparative analysis (Figs. 5 and 6) to understand the relationship between mRNA and protein

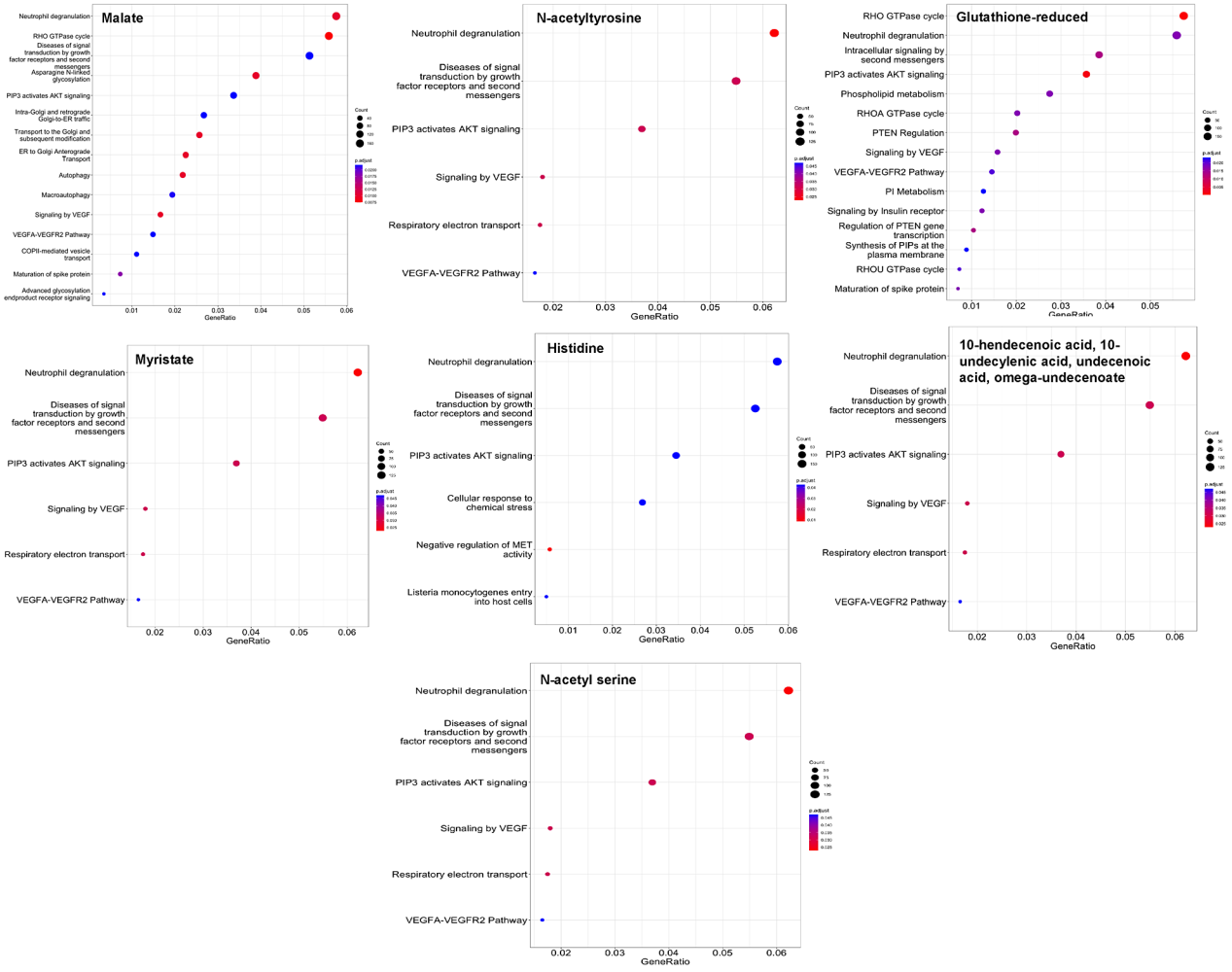

Fig. 8 Seven enriched pathways from co-expression analysis associated with compounds involving Neutrophil degranulation: Malate, N-acetyltyrosine, glutathione reduced, Myristate, Histidine, undecenoic acid, and N-acetylserine. Cell pellets were pooled from $n=6$ wells/ condition for metabolomic analysis

expression levels by comparing gene expression data obtained from RNA-seq with protein levels determined through mass spectrometry (MS). Proteins were isolated from the extracellular matrix that was synthesized by SMCs and deposited in the culture wells (ECM), as well as from the cytosol (C) and cytoskeleton (CS) of cells. We observed a moderate yet statistically significant correlation between mRNA abundance as estimated by RNA-seq, and protein abundance as determined from MS. This correlation was quantified using Spearman's correlation coefficient (Rho), which ranged from 0.24 to 0.6 across various samples. These findings suggest that alterations at the transcriptional level are broadly reflected at the protein level, influencing biological pathways.

The correlation between mRNA and protein abundance has been widely debated, as it varies significantly depending on the biological context. Studies have demonstrated that the correlation between mRNA and protein under specific conditions can range from 0.09 to 0.57, based on Spearman's rank correlations [71]. In our data, the Spearman's rank correlation between mRNA and protein ranges from 0.2 to 0.6, which is consistent with this typical range. While the relationship between mRNA and protein is context-dependent and complex, it does not necessarily mean that mRNA findings cannot inform protein levels. Rather, mRNA and proteins represent distinct regulatory layers, and protein abundance can be inferred from mRNA levels – not through direct correlation but using machine learning models that account for these intricate relationships [72].

Identifying metabolites co-expressed genes and enriched pathways

Gene expressions and metabolites constitute two distinct layers of features that can characterize dynamic responses to changes in glucose levels. We investigated

which genes are co-expressed with metabolites. For each metabolite, we identified gene sets that exhibited similar dynamic patterns, using Spearman's rank correlation coefficient (Rho) with a threshold of |Rho| > 0.9. Subsequently, we conducted a pathway enrichment analysis to determine which pathways are enriched in these co-expressed gene modules, which show similar patterns to the metabolites.

Notably, the L13a-mediated translational silencing pathway and the neutrophil degranulation pathway were repeatedly found to be enriched, linked to genes co-expressed with 9 and 7 different compounds respectively, as depicted in Figs. 7 and 8. The L13a pathway plays a crucial role in cellular stress responses and could potentially reduce inflammation triggered by elevated glucose levels by regulating the translation of pro-inflammatory cytokines, thus acting as a defense mechanism against stress induced by hyperglycemia. Meanwhile, the neutrophil degranulation pathway, crucial for immune defense through the release of enzymes and reactive substances, might aggravate tissue damage under hyperglycemic conditions by promoting neutrophil activation and degranulation. These findings suggest that metabolites induced by hyperglycemia can indirectly indicate immune response signals, as inferred through pathway enrichment analysis using co-expressed genes with metabolites. A comprehensive list of enriched pathways associated with each metabolite's co-expressed genes is presented in Table S2.

Among the compounds involving L13a-mediated translational silencing of ceruloplasmin expression (Fig. 7), proline and picolinate are interesting. For instance, proline elevation is associated with lactic acidosis, and plasma proline levels strongly correlate with hemoglobin A1c and insulin-related variables (e.g., C-peptide, insulin, HOMA-IR) [73], although dietary proline intake was not significantly associated with T2DM in an adult cohort study [74]. Picolinic acid, on the other hand, is an efficient chelator, and chromium picolinate has been promoted as a dietary supplement for T2DM patients owing to its role in blood glucose regulation, carbohydrate and lipid metabolism, and body composition [75].

In a similar vein, prior studies have shown that high glucose and inflammatory conditions coax primary aortic SMCs to express higher levels of G6PDH and NADPH oxidase, elevated pentose phosphate pathway activity, and upper glycolysis pathway [76, 77]. Other pathways that are enhanced in SMCs under hyperglycemic conditions include protein kinase C signaling, RAGE (receptor for advanced glycation end products)/ERK/NF-κB signaling pathway, and ERK/Akt signaling pathway, which contribute to increased formation and accumulation of AGEs, progression of atherosclerosis and vascular calcification, induction of iNOS activity, autophagy, and VSMC proliferation, among others [50].

Limitations of this study

While our study extends human SMC exposure to hyperglycemia in vitro from acute (typically < 72 h) to chronic (3-week culture) culture, diabetes develops over a long period in vivo, sometimes over decades, which would be hard to replicate in vitro. T2DM is a complicated process involving interactions between multiple cell types, and hyperglycemia is perhaps just one of the contributors to this condition, which warrants further in vitro investigations on other contributors. For these findings to be relevant to human T2DM, selected studies in animal models are required to elucidate the mechanisms involved and identify possible therapeutic applications. Furthermore, our in vitro results should be validated in other healthy and T2DM patient derived SMCs in vitro, and in vivo in future studies.

Conclusions

This study investigates the effects of hyperglycemic condition on human aortic SMCs cultured under varying glucose concentrations (5 mmol/L, 10 mmol/L, 20 mmol/L), and compared to SMCs isolated from patients with type 2 diabetes (T2DM). We noted that chronic hyperglycemia, in a glucose concentration dependent manner, induced significant changes within human SMCs in vitro in their (i) phenotype and biophysical characteristics, (ii) biomechanical properties (Young's modulus, membrane tension, tether and adhesion forces), (iii) cytokines/ chemokines/ growth factors/ and MMPs-TIMPs release, and (iv) differential expressions in gene-sets and pathways representing inflammation, matrix turnover, and metabolic pathways. The biomechanical results (F_T, F_{ad}, T_M and R_T) presented here for human T2DM cells and those of human SMCs under hyperglycemic conditions haven't been reported earlier in literature. Our integrated analysis of omics datasets revealed specific biomarkers and enriched pathways, which we report for the first time on T2DM cells and on human SMCs receiving higher glucose levels, furthering our knowledge on chronic hyperglycemia-induced changes in arterial remodeling and their complex relationships.

Abbreviations

AFM	Atomic force microscopy
T2DM	Type 2 diabetes mellitus
CVD	cardiovascular diseases
VEGF	vascular endothelial growth factor
NO	nitric oxide
VSMCs	Vascular smooth muscle cells
ECs	Endothelial cells
GAGs	glycosaminoglycans
IGF	Insulin-like growth factor
ECM	Extracellular matrix
ROS	Reactive oxygen species
NF-kappaB	nuclear factor kappaB
RAGE	Receptor for advanced glycation end-products
FAK	Focal adhesion kinase
MMP-2	Matrix metalloproteinase-2

ICAM-1	Intercellular cell adhesion molecule-1
VCAM-1	Vascular cell adhesion molecule-1
HAOSMC	Human aortic smooth muscle cells
T2DM-HAOSMCs	Type II diabetic patients derived aortic smooth muscle cells

Supplementary Information

The online version contains supplementary material available at https://doi.org/10.1186/s13036-024-00457-w.

Supplementary Material 1

Supplementary Material 2

Acknowledgements
We acknowledge access to the Mass Spectrometry facility in the Department of Chemistry at Cleveland State University. We would like to express our gratitude to the Genomics Core at Cleveland Clinic for their invaluable assistance with library preparation and sequencing.

Author contributions
CK: conceptualization, formal analysis, funding acquisition, project administration, supervision, writing original draft, review and editing. PJ: funding acquisition, computational analysis, methodology, supervision, writing original draft, review and editing. SB: experimental design, formal analysis, methodology, writing original draft. AB: computational analysis, methodology. YS: methodology, metabolomics, supervision, manuscript editing and review. IR: metabolomics, experimental setup and data analysis. EGE: atomic force microscopy, data acquisition and analysis.

Funding
NHLBI/NIH Progenitor Cell Translational Consortium (PCTC) (MIRC-002500: to PJ) and Defense Advanced Research Projects Agency (DARPA) (AWD00001593: to PJ); Partial support from National Science Foundation (NSF) grants 1927602 and 1337859 to CK; and the Cellular and Molecular Medicine Fellowship from Cleveland State University to SB.

Data availability
No datasets were generated or analysed during the current study.

Declarations

Ethics approval and consent to participate
Not applicable.

Consent for publication
Not applicable.

Competing interests
The authors declare no competing interests.

Author details
[1]Department of Chemical and Biomedical Engineering, Cleveland State University, Cleveland, OH 44115, USA
[2]Department of Biological, Geological and Environmental Sciences, Cleveland State University, Cleveland, OH 44115, USA
[3]Department of Chemistry, Cleveland State University, Cleveland, OH 44115, USA
[4]Center for Gene Regulation in Health and Disease, Cleveland State University, Cleveland, OH 44115, USA
[5]Center for RNA Science and Therapeutics, School of Medicine, Case Western Reserve University, 10900 Euclid Avenue, Cleveland, OH 44106, USA

Received: 14 June 2024 / Accepted: 14 October 2024
Published online: 29 October 2024

References

1. Khan MAB, Hashim MJ, King JK, Govender RD, Mustafa H, Al Kaabi J. Epidemiology of type 2 diabetes - global burden of Disease and Forecasted trends. J Epidemiol Glob Health. 2020;10(1):107–11. https://doi.org/10.2991/jegh.k.191028.001.
2. De Rosa S, Arcidiacono B, Chiefari E, Brunetti A, Indolfi C, Foti DP. Type 2 diabetes Mellitus and Cardiovascular Disease: genetic and epigenetic links. Front Endocrinol (Lausanne). 2018;9:2. https://doi.org/10.3389/fendo.2018.00002.
3. Martín-Timón I, Sevillano-Collantes C, Segura-Galindo A, Del Cañizo-Gómez FJ. Type 2 diabetes and cardiovascular disease: have all risk factors the same strength? World J Diabetes. 2014;5(4):444–70. https://doi.org/10.4239/wjd.v5.i4.444.
4. Einarson TR, Acs A, Ludwig C, Panton UH. Prevalence of cardiovascular disease in type 2 diabetes: a systematic literature review of scientific evidence from across the world in 2007–2017. Cardiovasc Diabetol. 2018;17(1):83. https://doi.org/10.1186/s12933-018-0728-6.
5. Assar ME, Angulo J, Rodríguez-Mañas L. Diabetes and ageing-induced vascular inflammation. J Physiol. 2016;594(8):2125–46. https://doi.org/10.1113/JP270841.
6. Halter JB, Musi N, McFarland Horne F, Crandall JP, Goldberg A, Harkless L, Hazzard WR, Huang ES, Kirkman MS, Plutzky J, et al. Diabetes and cardiovascular disease in older adults: current status and future directions. Diabetes. 2014;63(8):2578–89. https://doi.org/10.2337/db14-0020.
7. Zheng M, Zhang X, Chen S, Song Y, Zhao Q, Gao X, Wu S. Arterial stiffness preceding diabetes: a longitudinal study. Circ Res. 2020;127(12):1491–8. https://doi.org/10.1161/CIRCRESAHA.120.317950.
8. Gast KB, Tjeerdema N, Stijnen T, Smit JW, Dekkers OM. Insulin resistance and risk of incident cardiovascular events in adults without diabetes: meta-analysis. PLoS ONE. 2012;7(12):e52036. https://doi.org/10.1371/journal.pone.0052036.
9. Laakso M, Kuusisto J. Insulin resistance and hyperglycaemia in cardiovascular disease development. Nat Rev Endocrinol. 2014;10(5):293–302. https://doi.org/10.1038/nrendo.2014.29.
10. Nordestgaard BG, Varbo A. Triglycerides and cardiovascular disease. Lancet. 2014;384(9943):626–35. https://doi.org/10.1016/S0140-6736(14)61177-6.
11. Roberts AC, Porter KE. Cellular and molecular mechanisms of endothelial dysfunction in diabetes. Diab Vasc Dis Res. 2013;10(6):472–82. https://doi.org/10.1177/1479164113500680.
12. Tabit CE, Chung WB, Hamburg NM, Vita JA. Endothelial dysfunction in diabetes mellitus: molecular mechanisms and clinical implications. Rev Endocr Metab Disord. 2010;11(1):61–74. https://doi.org/10.1007/s11154-010-9134-4.
13. Galicia-Garcia U, Benito-Vicente A, Jebari S, Larrea-Sebal A, Siddiqi H, Uribe KB, Ostolaza H, Martín C. Pathophysiology of type 2 diabetes Mellitus. Int J Mol Sci. 2020;21(17). https://doi.org/10.3390/ijms21176275.
14. Rask-Madsen C, King GL. Vascular complications of diabetes: mechanisms of injury and protective factors. Cell Metab. 2013;17(1):20–33. https://doi.org/10.1016/j.cmet.2012.11.012.
15. Bergandi L, Silvagno F, Russo I, Riganti C, Anfossi G, Aldieri E, Ghigo D, Trovati M, Bosia A. Insulin stimulates glucose transport via nitric oxide/cyclic GMP pathway in human vascular smooth muscle cells. Arterioscler Thromb Vasc Biol. 2003;23(12):2215–21. https://doi.org/10.1161/01.ATV.0000107028.20478.8e.
16. Nieves-Cintrón M, Flores-Tamez VA, Le T, Baudel MM, Navedo MF. Cellular and molecular effects of hyperglycemia on ion channels in vascular smooth muscle. Cell Mol Life Sci. 2021;78(1):31–61. https://doi.org/10.1007/s00018-020-03582-z.
17. Xi G, Shen X, Wai C, White MF, Clemmons DR. Hyperglycemia induces vascular smooth muscle cell dedifferentiation by suppressing insulin receptor substrate-1-mediated p53/KLF4 complex stabilization. J Biol Chem. 2019;294(7):2407–21. https://doi.org/10.1074/jbc.RA118.005398.
18. Tong X, Ying J, Pimentel DR, Trucillo M, Adachi T, Cohen RA. High glucose oxidizes SERCA cysteine-674 and prevents inhibition by nitric oxide of smooth muscle cell migration. J Mol Cell Cardiol. 2008;44(2):361–9. https://doi.org/10.1016/j.yjmcc.2007.10.022.
19. Hattori Y, Hattori S, Sato N, Kasai K. High-glucose-induced nuclear factor kappaB activation in vascular smooth muscle cells. Cardiovasc Res. 2000;46(1):188–97. https://doi.org/10.1016/s0008-6363(99)00425-3.
20. Peiró C, Lafuente N, Matesanz N, Cercas E, Llergo JL, Vallejo S, Rodríguez-Mañas L, Sánchez-Ferrer CF. High glucose induces cell death of cultured human aortic smooth muscle cells through the formation of hydrogen peroxide. Br J Pharmacol. 2001;133(7):967–74. https://doi.org/10.1038/sj.bjp.0704184.

21. Ramana KV, Tammali R, Reddy AB, Bhatnagar A, Srivastava SK. Aldose reductase-regulated tumor necrosis factor-alpha production is essential for high glucose-induced vascular smooth muscle cell growth. Endocrinology. 2007;148(9):4371–84. https://doi.org/10.1210/en.2007-0512.
22. Su SC, Hung YJ, Huang CL, Shieh YS, Chien CY, Chiang CF, Liu JS, Lu CH, Hsieh CH, Lin CM, et al. Cilostazol inhibits hyperglucose-induced vascular smooth muscle cell dysfunction by modulating the RAGE/ERK/NF-κB signaling pathways. J Biomed Sci. 2019;26(1):68. https://doi.org/10.1186/s12929-019-0550-9.
23. Little PJ, Osman N, de Dios ST, Cemerlang N, Ballinger M, Nigro J. Anti-proliferative activity of oral anti-hyperglycemic agents on human vascular smooth muscle cells: thiazolidinediones (glitazones) have enhanced activity under high glucose conditions. Cardiovasc Diabetol. 2007;6:33. https://doi.org/10.1186/1475-2840-6-33.
24. Güemes M, Rahman SA, Hussain K. What is a normal blood glucose? Arch Dis Child. 2016;101(6):569–74. https://doi.org/10.1136/archdischild-2015-308336.
25. Association AD. 2. Classification and diagnosis of diabetes. Diabetes Care. 2018;41(Suppl 1):S13–27. https://doi.org/10.2337/dc18-S002.
26. Patterson C, Mapera S, Li HH, Madamanchi N, Hilliard E, Lineberger R, Hermann R, Charles P. Comparative effects of paclitaxel and rapamycin on smooth muscle migration and survival: role of AKT-dependent signaling. Arterioscler Thromb Vasc Biol. 2006;26(7):1473–80. https://doi.org/10.1161/01.ATV.0000223866.42883.3b.
27. Mankovich N, Kehoe E, Peterson A, Kirby M. Pathway expression analysis. Sci Rep. 2022;12(1):21839. https://doi.org/10.1038/s41598-022-26381-x.
28. Farrell K, Borazjani A, Damaser M, Kothapalli CR. Differential regulation of NSC phenotype and genotype by chronically activated microglia within cocultures. Integr Biol (Camb). 2016;8(11):1145–57. https://doi.org/10.1039/c6ib00126b.
29. Dudiki T, Mahajan G, Liu H, Zhevlakova I, Bertagnolli C, Nascimento DW, Kothapalli CR, Byzova TV. Kindlin3 regulates biophysical properties and mechanics of membrane to cortex attachment. Cell Mol Life Sci. 2021;78(8):4003–18. https://doi.org/10.1007/s00018-021-03817-7.
30. Langmead B, Trapnell C, Pop M, Salzberg SL. Ultrafast and memory-efficient alignment of short DNA sequences to the human genome. Genome Biol. 2009;10(3):R25. https://doi.org/10.1186/gb-2009-10-3-r25.
31. Li B, Dewey CN. RSEM: accurate transcript quantification from RNA-Seq data with or without a reference genome. BMC Bioinformatics. 2011;12:323. https://doi.org/10.1186/1471-2105-12-323.
32. Leng N, Dawson JA, Thomson JA, Ruotti V, Rissman AI, Smits BM, Haag JD, Gould MN, Stewart RM, Kendziorski C. EBSeq: an empirical Bayes hierarchical model for inference in RNA-seq experiments. Bioinformatics. 2013;29(8):1035–43. https://doi.org/10.1093/bioinformatics/btt087. From NLM Medline.
33. Yu G, He QY. ReactomePA: an R/Bioconductor package for reactome pathway analysis and visualization. Mol Biosyst. 2016;12(2):477–9. https://doi.org/10.1039/c5mb00663e. From NLM Medline.
34. Faries PL, Rohan DI, Takahara H, Wyers MC, Contreras MA, Quist WC, King GL, Logerfo FW. Human vascular smooth muscle cells of diabetic origin exhibit increased proliferation, adhesion, and migration. J Vasc Surg. 2001;33(3):601–7. https://doi.org/10.1067/mva.2001.111806.
35. Shen JY, Chan-Park MB, He B, Zhu AP, Zhu X, Beuerman RW, Yang EB, Chen W, Chan V. Three-dimensional microchannels in biodegradable polymeric films for control orientation and phenotype of vascular smooth muscle cells. Tissue Eng. 2006;12(8):2229–40. https://doi.org/10.1089/ten.2006.12.2229.
36. Chang S, Song S, Lee J, Yoon J, Park J, Choi S, Park JK, Choi K, Choi C. Phenotypic modulation of primary vascular smooth muscle cells by short-term culture on micropatterned substrate. PLoS ONE. 2014;9(2):e88089. https://doi.org/10.1371/journal.pone.0088089.
37. Farrell K, Simmers P, Mahajan G, Boytard L, Camardo A, Joshi J, Ramamurthi A, Pinet F, Kothapalli CR. Alterations in phenotype and gene expression of adult human aneurysmal smooth muscle cells by exogenous nitric oxide. Exp Cell Res. 2019;384(1):111589. https://doi.org/10.1016/j.yexcr.2019.111589.
38. McCallinhart PE, Cho Y, Sun Z, Ghadiali S, Meininger GA, Trask AJ. Reduced stiffness and augmented traction force in type 2 diabetic coronary microvascular smooth muscle. Am J Physiol Heart Circ Physiol. 2020;318(6):H1410–9. https://doi.org/10.1152/ajpheart.00542.2019.
39. Diz-Muñoz A, Fletcher DA, Weiner OD. Use the force: membrane tension as an organizer of cell shape and motility. Trends Cell Biol. 2013;23(2):47–53. https://doi.org/10.1016/j.tcb.2012.09.006.
40. Hochmuth FM, Shao JY, Dai J, Sheetz MP. Deformation and flow of membrane into tethers extracted from neuronal growth cones. Biophys J. 1996;70(1):358–69. https://doi.org/10.1016/S0006-3495(96)79577-2.
41. Bastola S, Kothapalli C, Ramamurthi A. Sodium Nitroprusside Stimulation of Elastic Matrix regeneration by Aneurysmal Smooth Muscle Cells. Tissue Eng Part A. 2023;29(7–8):225–43. https://doi.org/10.1089/ten.TEA.2022.0169.
42. Gupta C, Tikoo K. High glucose and insulin differentially modulates proliferation in MCF-7 and MDA-MB-231 cells. J Mol Endocrinol. 2013;51(1):119–29. https://doi.org/10.1530/JME-13-0062.
43. Jeong IK, Oh DH, Park SJ, Kang JH, Kim S, Lee MS, Kim MJ, Hwang YC, Ahn KJ, Chung HY, et al. Inhibition of NF-κB prevents high glucose-induced proliferation and plasminogen activator inhibitor-1 expression in vascular smooth muscle cells. Exp Mol Med. 2011;43(12):684–92. https://doi.org/10.3858/emm.2011.43.12.079.
44. Wang K, Deng X, Shen Z, Jia Y, Ding R, Li R, Liao X, Wang S, Ha Y, Kong Y, et al. High glucose promotes vascular smooth muscle cell proliferation by upregulating proto-oncogene serine/threonine-protein kinase Pim-1 expression. Oncotarget. 2017;8(51):88320–31. https://doi.org/10.18632/oncotarget.19368.
45. P Chen G, Q Zhang X, Wu T, Li L, Han J, Q Du C. Alteration of mevalonate pathway in proliferated vascular smooth muscle from diabetic mice: possible role in high-glucose-induced atherogenic process. J Diabetes Res. 2015;2015(379287). https://doi.org/10.1155/2015/379287.
46. Zhu Y, Liu X, Xu Y, Lin Y. Hyperglycemia disturbs trophoblast functions and subsequently leads to failure of uterine spiral artery remodeling. Front Endocrinol (Lausanne). 2023;14:1060253. https://doi.org/10.3389/fendo.2023.1060253.
47. Kozakova M, Morizzo C, Bianchi C, Di Filippi M, Miccoli R, Paterni M, Di Bello V, Palombo C. Glucose-related arterial stiffness and carotid artery remodeling: a study in normal subjects and type 2 diabetes patients. J Clin Endocrinol Metab. 2014;99(11):E2362–2366. https://doi.org/10.1210/jc.2014-2028.
48. Yahagi K, Kolodgie FD, Lutter C, Mori H, Romero ME, Finn AV, Virmani R. Pathology of Human Coronary and Carotid Artery atherosclerosis and vascular calcification in diabetes Mellitus. Arterioscler Thromb Vasc Biol. 2017;37(2):191–204. https://doi.org/10.1161/ATVBAHA.116.306256.
49. Lin PK, Davis GE. Extracellular matrix remodeling in Vascular Disease: defining its regulators and pathological influence. Arterioscler Thromb Vasc Biol. 2023;43(9):1599–616. https://doi.org/10.1161/ATVBAHA.123.318237.
50. Shi J, Yang Y, Cheng A, Xu G, He F. Metabolism of vascular smooth muscle cells in vascular diseases. Am J Physiol Heart Circ Physiol. 2020;319(3):H613–31. https://doi.org/10.1152/ajpheart.00220.2020.
51. Pickup JC, Chusney GD, Thomas SM, Burt D. Plasma interleukin-6, tumour necrosis factor alpha and blood cytokine production in type 2 diabetes. Life Sci. 2000;67(3):291–300. https://doi.org/10.1016/s0024-3205(00)00622-6.
52. Esposito K, Nappo F, Marfella R, Giugliano G, Giugliano F, Ciotola M, Quagliaro L, Ceriello A, Giugliano D. Inflammatory cytokine concentrations are acutely increased by hyperglycemia in humans: role of oxidative stress. Circulation. 2002;106(16):2067–72. https://doi.org/10.1161/01.cir.0000034509.14906.ae.
53. Freitas Lima LC, Braga VA, Silva M, Cruz JC, Sousa Santos SH, de Oliveira Monteiro MM, Balarini CM. Adipokines, diabetes and atherosclerosis: an inflammatory association. Front Physiol. 2015;6:304. https://doi.org/10.3389/fphys.2015.00304.
54. Lindschau C, Quass P, Menne J, Güler F, Fiebeler A, Leitges M, Luft FC, Haller H. Glucose-induced TGF-beta1 and TGF-beta receptor-1 expression in vascular smooth muscle cells is mediated by protein kinase C-alpha. Hypertension. 2003;42(3):335–41. https://doi.org/10.1161/01.HYP.0000087839.72582.DD.
55. Benjamin LE, Glucose. VEGF-A, and diabetic complications. Am J Pathol. 2001;158(4):1181–4. https://doi.org/10.1016/S0002-9440(10)64066-7.
56. Macarie RD, Vadana M, Ciortan L, Tucureanu MM, Ciobanu A, Vinereanu D, Manduteanu I, Simionescu M, Butoi E. The expression of MMP-1 and MMP-9 is up-regulated by smooth muscle cells after their cross-talk with macrophages in high glucose conditions. J Cell Mol Med. 2018;22(9):4366–76. https://doi.org/10.1111/jcmm.13728.
57. Virmani R, Burke AP, Kolodgie F. Morphological characteristics of coronary atherosclerosis in diabetes mellitus. *Can J Cardiol* 2006, *22 Suppl B* (Suppl B), 81B-84B. https://doi.org/10.1016/s0828-282x(06)70991-6
58. Kologrivova IV, Suslova TE, Koshel'skaya OA, Vinnitskaya IV, Trubacheva OA. System of matrix metalloproteinases and cytokine secretion in type 2 diabetes mellitus and impaired carbohydrate tolerance associated with arterial hypertension. Bull Exp Biol Med. 2014;156(5):635–8. https://doi.org/10.1007/s10517-014-2413-4.

59. Fiorentino L, Cavalera M, Menini S, Marchetti V, Mavilio M, Fabrizi M, Conserva F, Casagrande V, Menghini R, Pontrelli P, et al. Loss of TIMP3 underlies diabetic nephropathy via FoxO1/STAT1 interplay. EMBO Mol Med. 2013;5(3):441–55. https://doi.org/10.1002/emmm.201201475.
60. Yundung Y, Mohammed S, Paneni F, Reutersberg B, Rössler F, Zimmermann A, Pelisek J. Transcriptomics analysis of long non-coding RNAs in smooth muscle cells from patients with peripheral artery disease and diabetes mellitus. Sci Rep. 2024;14(1):8615. https://doi.org/10.1038/s41598-024-59164-7.
61. Soundararajan M, Willard FS, Kimple AJ, Turnbull AP, Ball LJ, Schoch GA, Gileadi C, Fedorov OY, Dowler EF, Higman VA, et al. Structural diversity in the RGS domain and its interaction with heterotrimeric G protein alpha-subunits. Proc Natl Acad Sci U S A. 2008;105(17):6457–62. https://doi.org/10.1073/pnas.0801508105.
62. Ma YC, Huang J, Ali S, Lowry W, Huang XY. Src tyrosine kinase is a novel direct effector of G proteins. Cell. 2000;102(5):635–46. https://doi.org/10.1016/s0092-8674(00)00086-6.
63. Akhtar S, Benter IF. The role of epidermal growth factor receptor in diabetes-induced cardiac dysfunction. Bioimpacts. 2013;3(1):5–9. https://doi.org/10.5681/bi.2013.008.
64. Wagenseil JE, Mecham RP. Vascular extracellular matrix and arterial mechanics. Physiol Rev. 2009;89(3):957–89. https://doi.org/10.1152/physrev.00041.2008.
65. Cocciolone AJ, Hawes JZ, Staiculescu MC, Johnson EO, Murshed M, Wagenseil JE. Elastin, arterial mechanics, and cardiovascular disease. Am J Physiol Heart Circ Physiol. 2018;315(2):H189–205. https://doi.org/10.1152/ajpheart.00087.2018.
66. Song W, Ergul A. Type-2 diabetes-induced changes in vascular extracellular matrix gene expression: relation to vessel size. Cardiovasc Diabetol. 2006;5:3. https://doi.org/10.1186/1475-2840-5-3.
67. DeMarsilis AJ, Walji TA, Maedeker JA, Stoka KV, Kozel BA, Mecham RP, Wagenseil JE, Craft CS. Elastin Insufficiency predisposes mice to impaired glucose metabolism. J Mol Genet Med. 2014;8(3). https://doi.org/10.4172/1747-0862.1000129.
68. Cangemi C, Skov V, Poulsen MK, Funder J, Twal WO, Gall MA, Hjortdal V, Jespersen ML, Kruse TA, Aagard J, et al. Fibulin-1 is a marker for arterial extracellular matrix alterations in type 2 diabetes. Clin Chem. 2011;57(11):1556–65. https://doi.org/10.1373/clinchem.2011.162966.
69. Song G, Lin D, Bao L, Jiang Q, Zhang Y, Zheng H, Gao Q. Effects of high glucose on the expression of LAMA1 and Biological Behavior of Choroid Retinal endothelial cells. J Diabetes Res. 2018;2018(7504614). https://doi.org/10.1155/2018/7504614.
70. Zhu H, Zhu X, Liu Y, Jiang F, Chen M, Cheng L, Cheng X. Gene expression profiling of type 2 diabetes Mellitus by Bioinformatics Analysis. Comput Math Methods Med. 2020;2020:9602016. https://doi.org/10.1155/2020/9602016.
71. Pascal LE, True LD, Campbell DS, Deutsch EW, Risk M, Coleman IM, Eichner LJ, Nelson PS, Liu AY. Correlation of mRNA and protein levels: cell type-specific gene expression of cluster designation antigens in the prostate. BMC Genomics. 2008;9:246. https://doi.org/10.1186/1471-2164-9-246.
72. Prabahar A, Zamora R, Barclay D, Yin J, Ramamoorthy M, Bagheri A, Johnson SA, Badylak S, Vodovotz Y, Jiang P. Unraveling the complex relationship between mRNA and protein abundances: a machine learning-based approach for imputing protein levels from RNA-seq data. NAR Genom Bioinform. 2024;6(1):lqae019. https://doi.org/10.1093/nargab/lqae019.
73. Nakamura H, Jinzu H, Nagao K, Noguchi Y, Shimba N, Miyano H, Watanabe T, Iseki K. Plasma amino acid profiles are associated with insulin, C-peptide and adiponectin levels in type 2 diabetic patients. Nutr Diabetes. 2014;4(9). https://doi.org/10.1038/nutd.2014.32. e133.
74. Najafi F, Mohseni P, Pasdar Y, Niknam M, Izadi N. The association between dietary amino acid profile and the risk of type 2 diabetes: Ravansar non-communicable disease cohort study. BMC Public Health. 2023;23(1):2284. https://doi.org/10.1186/s12889-023-17210-5.
75. Paiva AN, Lima JG, Medeiros AC, Figueiredo HA, Andrade RL, Ururahy MA, Rezende AA, Brandão-Neto J, Almeida M. Beneficial effects of oral chromium picolinate supplementation on glycemic control in patients with type 2 diabetes: a randomized clinical study. J Trace Elem Med Biol. 2015;32:66–72. https://doi.org/10.1016/j.jtemb.2015.05.006.
76. Alamri A, Burzangi AS, Coats P, Watson DG. Untargeted Metabolic Profiling Cell-Based Approach of Pulmonary Artery Smooth Muscle Cells in Response to High Glucose and the Effect of the Antioxidant Vitamins D and E. *Metabolites* 2018, *8* (4). https://doi.org/10.3390/metabo8040087
77. Peiró C, Romacho T, Azcutia V, Villalobos L, Fernández E, Bolaños JP, Moncada S, Sánchez-Ferrer CF. Inflammation, glucose, and vascular cell damage: the role of the pentose phosphate pathway. Cardiovasc Diabetol. 2016;15:82. https://doi.org/10.1186/s12933-016-0397-2.

Publisher's note